2 Hyperspectral Assessment of Ecophysiological Functioning for Diagnostics of Crops and Vegetation

Yoshio Inoue, Roshanak Darvishzadeh, and Andrew Skidmore

CONTENTS

2.1 INTRODUCTION

Ecophysiological functioning of vegetation is an essential basis for plant production, food security, and carbon exchange between land surface and the atmosphere. Plant productivity varies to a large extent based on the ecophysiological functioning under changing environment and management. Carbon and water balances in ecosystems are strongly controlled by ecophysiological functioning such as photosynthesis and transpiration (Nobel, 2005).

Accordingly, systematic monitoring, assessment, and prediction of the ecophysiological functioning in various scales are critical for food security and environmental policy making. Geospatial information on crop growth and ecophysiological functioning is useful for site-specific management and smart agriculture that seek to achieve higher crop yield and quality with less labor and agrochemical inputs. Regional or global scale information on plant growth, carbon exchange, and water balance would support policy making for better management of ecosystems and environment (de Leeuw et al., 2010; Vadrevu et al., 2018).

Assessment of photosynthetic functioning is one of the most important bases for the diagnosis and prediction of plant growth, as well as carbon exchange between ecosystems and the atmosphere. A great deal of research effort has been directed toward the assessment of ecophysiological variables and plant productivity using remote sensing in optical, thermal, and microwave wavelength domains together with modeling approaches (e.g., reviews by Moran et al., 1997; Inoue, 2003; Olioso et al., 2005). Remotely sensed optical signatures have proven useful for estimating ecological variables such as leaf area index (LAI) and the absorptivity of photosynthetically active radiation (fAPAR) that affect photosynthetic capacity (Daughtry et al., 1983; Asrar et al., 1989; Huete, 1988). Thermal remote sensing (e.g., brightness temperature) provides critical information on transpiration and/or water stress via energy balance of vegetation (Jackson et al., 1981; Inoue et al., 1990; Moran et al., 1994). Microwave signatures (e.g., backscattering coefficient) can provide structural information of plant canopies such as leaf area index and biomass depending on their frequency and incidence angle (Le Toan et al., 1997; Inoue et al., 2002; Inoue et al., 2014).

Nevertheless, the hyperspectral spectral reflectance in the optical domain is the richest information source for ecophysiological functioning owing to the close relationships of biophysical and biochemical properties of vegetation with the solar radiation (300–3300 nm). The typical seasonal change of hyperspectral reflectance in rice paddy (Figure 2.1) clearly depicts the spectral response to vegetation, water, and soil associated with plant growth. Such relationships are inherent because the biological properties, structures, and functions of vegetation would have been optimized in response to the high-resolution (~1 nm) spectral change of solar radiation for the survival strategies. Accordingly, hyperspectral reflectance data would provide various ecophysiological and biochemical information although the data richness is not always favorable for predictive purposes.

In this chapter, methodologies for and insights about the use of hyperspectral reflectance data for assessment of ecophysiological functioning are discussed based on a range of case studies with ground-based and airborne hyperspectral measurements.

2.2 LINKAGE OF ECOPHYSIOLOGICAL FUNCTIONING AND BIOPHYSICAL PROPERTIES WITH HYPERSPECTRAL REFLECTANCE

One of the most important functions of vegetation is photosynthesis. The net photosynthetic rate per leaf area (Pn) or net primary production (NPP) is the basis for plant production and crop yield. Photosynthesis is composed of several steps that work together in harmonized manner with high overall efficiency (Nobel, 2005). Pn is determined by (1) the photosynthetically active radiation absorbed by leaf chlorophyll (Chl-*a* and Chl-*b*); (2) water and carbon dioxide supplies; and (3) the photochemical and biochemical efficiency for producing carbohydrates. Accordingly, the amount of Chl-*a* and *b* provides essential information on the photons available for photosynthesis.

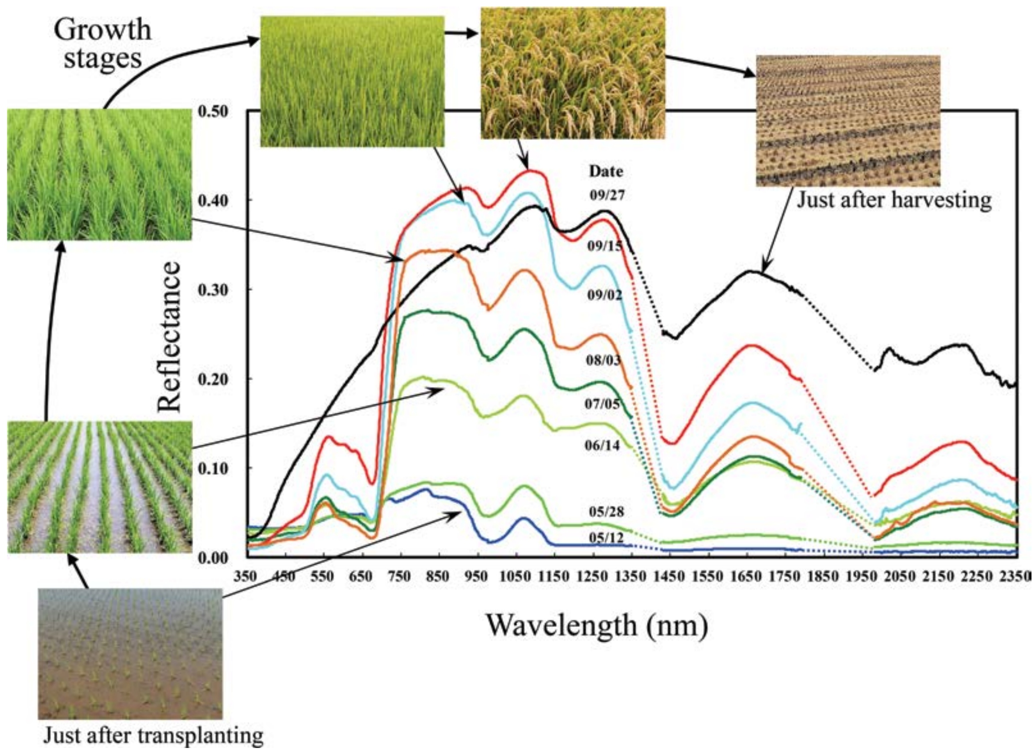

FIGURE 2.1 Typical seasonal change of hyperspectral reflectance in a rice paddy. Date (MM/DD) indicates month and date. Note: Spectral lines indicate the average spectrum of 10–30 measurements over individual canopy surfaces. Number of repetitions depends on the heterogeneity of each surface. This applies to all spectral lines for plant canopies throughout this chapter.

The de-epoxidation state of the xanthophyll cycle also provides physiological information on the photochemical activity related to heat dissipation (Demmig-Adams and Adams, 1996).

The absorptivity of pure Chl-*a* and *b* has unique spectrum in 400–700 nm wavelength regions; Chl-*a* and Chl-*b* have relatively narrow peaks in blue (430 nm and 455 nm) and red (662 nm and 644 nm), respectively (Nobel, 2005). In plant leaves, these peaks shift toward longer wavelengths by 10–30 nm due to the interactions between chlorophyll molecules and the surrounding molecules such as proteins and lipids in the chloroplast membranes as well as the adjacent water molecules. Accordingly, the actual absorption peak of plant leaves is usually 670–680 nm (Figure 2.2).

On the other hand, the photochemical functionality may be related to the spectral change around 531 nm because a small spectral shift is associated with the de-epoxidation state of the xanthophyll cycle (Gamon et al., 1992; Peñuelas et al., 1995). This is the biological basis for photochemical reflectance index (PRI), where the shift of absorption spectra between zeaxanthin and violaxanthin is assumed to be detected by the difference of reflectance at around 531 nm (Figure 2.3).

Water is another essential basis for ecophysiological functioning of vegetation, and has significant influences on the photosynthetic efficiency through stomatal conductance and photochemical processes (Nobel, 2005). Since water has broad light absorption bands around 1450 and 1950 nm, reflectance spectra of leaves is strongly affected by leaf water content (Figure 2.4, Inoue et al., 1993; Ceccato et al., 2002). Accordingly, the water conditions can be detected by broad-band multispectral data by such as NDWI (normalized difference water index) using shortwave infrared bands (Hunt and Rock, 1989). Additionally, several hyperspectral signatures such as R970 nm, first derivative at 1121 nm, and the spectral shift at approximately 2010 nm were also closely related to leaf water status (Inoue et al., 1993). Peñuelas and Inoue (1999) showed that the ratio of reflectance at 970 nm

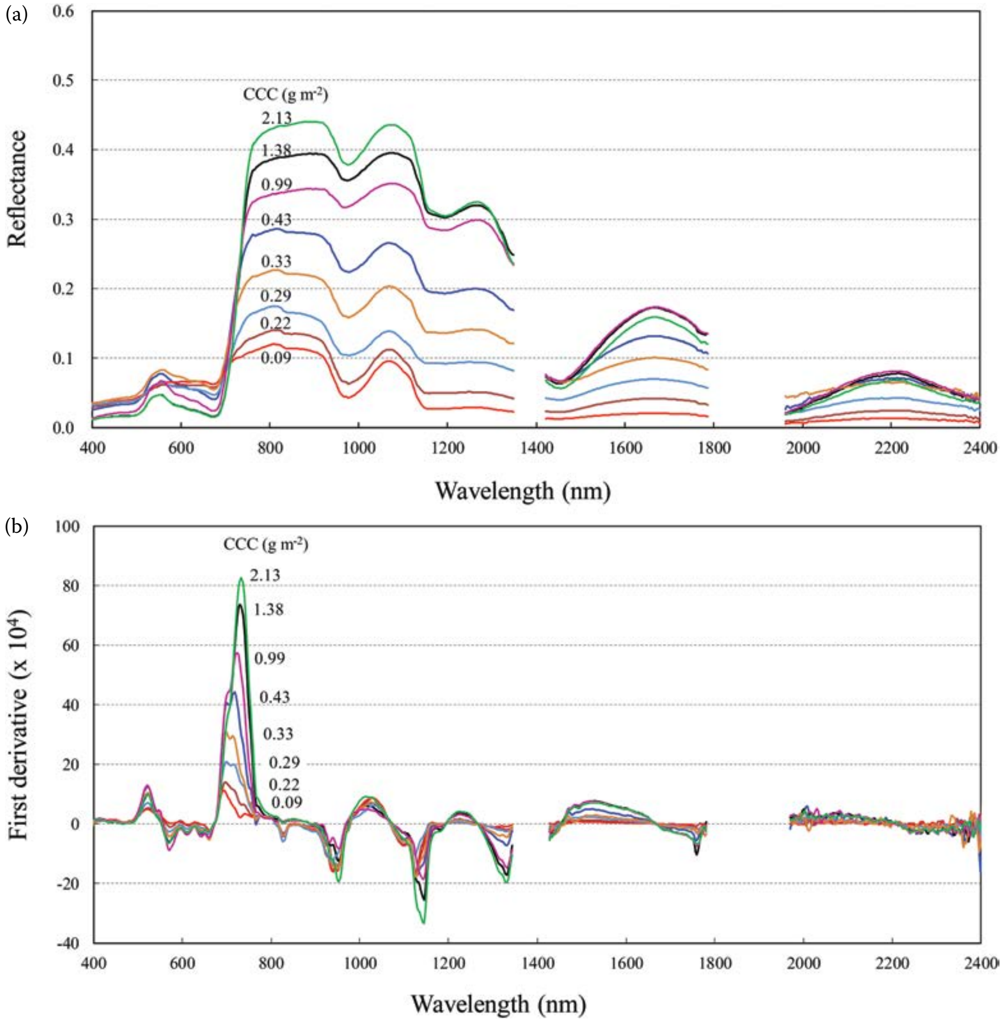

FIGURE 2.2 Typical reflectance spectra (a) and derivative spectra (b) for rice canopies with different canopy chlorophyll content (CCC). Data in two wavelength regions around 1400 and 1900 nm are eliminated because of the low incoming solar energy due to atmospheric water vapor. (After Inoue, Y. et al., 2016. *Plant, Cell and Environment*, 39, 2609–2623.)

(R_{970}) to R_{900} was closely correlated with leaf water condition. These findings would be useful for assessment of water stress of vegetation (Ceccato et al., 2002; Roberto et al., 2012).

Some additional spectral features related to specific pigments and biochemical functioning such as carotenoids, anthocyanin, and fluorescence would also be the basis for hyperspectral remote sensing of ecophysiological functioning (Blackburn, 1998; Gitelson et al., 2001; Grace et al., 2007). A number of researchers suggested that these signatures would be promising, although many more studies would be needed for accurate and robust monitoring of functioning of vegetation (Sims and Gamon, 2002; Ustin et al., 2009).

These unique spectral responses are the promising key for remote sensing of ecophysiological functioning of vegetation based on their inherent relations with the functioning. Hyperspectral measurement is necessary for detection and quantification of these spectral signatures since these narrow peaks can easily be masked or obscured in broad-band data. Especially in canopy or larger scales, subtle spectral changes associated with ecophysiological changes would also be obscured by

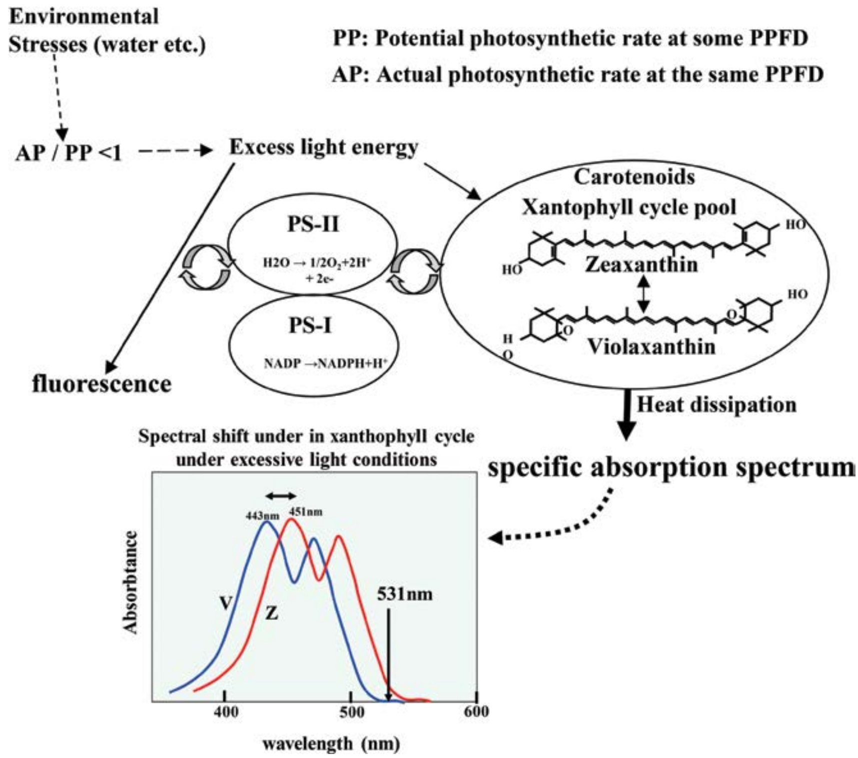

FIGURE 2.3 Schematic representation of spectral change associated with the xanthophyll cycle in response to environmental conditions.

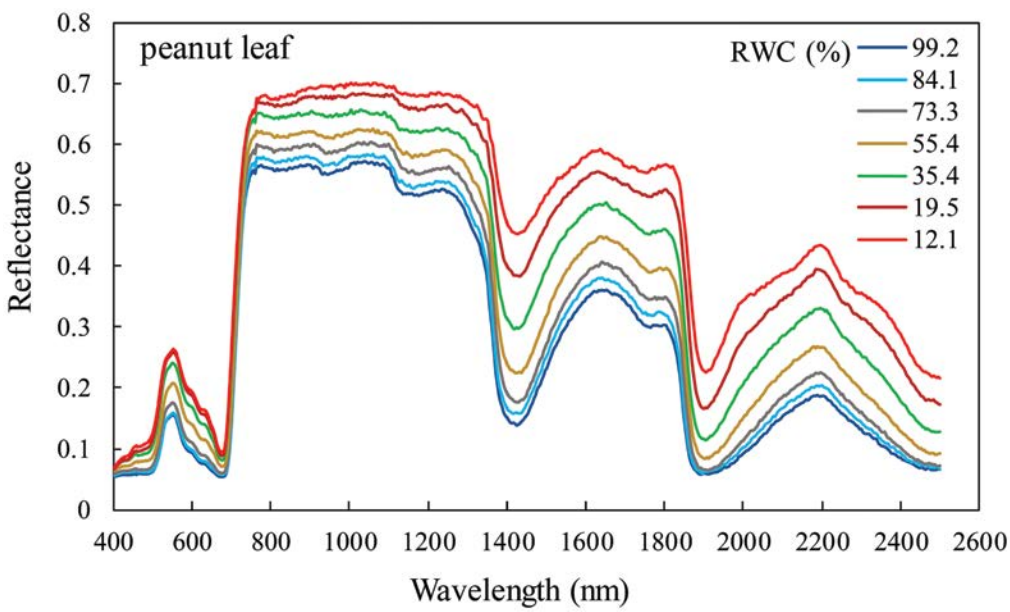

FIGURE 2.4 Typical change of reflectance spectra in response to relative water content (RWC) of a plant leaf. RWC is the ratio of actual water content to full-turgor water content. Each line indicates the single spectrum taken for a leaf with the corresponding RWC during consecutive desiccation.

various confounding factors such as canopy structure and background soils (Ceccato et al., 2002; Dash and Curran, 2004: Garbulsky et al., 2010).

2.3 METHODOLOGIES TO GENERATE PREDICTIVE MODELS FROM HYPERSPECTRAL DATA

It is essential to extract ecophysiological information from remotely sensed data for diagnostics and prediction of vegetation dynamics. A great deal of efforts have been spent to derive useful information from remotely sensed signatures. It is true that multispectral or broadband data can provide useful information on vegetation to some extent. Many vegetation indices have been developed for assessment of individual biophysical variables using multispectral data (Castro-Esau et al., 2006; Cammarano et al., 2014; Karnieli et al., 2013). However, hyperspectral datasets would provide much more opportunities for detection and modeling of ecophysiological, biochemical, and photochemical status due to the inherent linkages of narrow band signatures with ecophysiological functioning (see Section 2.2).

Additionally, hyperspectral data allow a range of advanced analytical methods such as derivative analysis, multivariable analysis, simulation for virtual sensor specification, and inversion of physically based models. Here, major methodologies enabled by hyperspectral measurement are discussed. Although they are semiempirical, data-driven, or physically based approaches, all types of methodologies are based on statistical or empirical modeling or parameterizations to a certain extent. Therefore, appropriate methodologies would have to be chosen for individual scientific or operational purposes.

2.3.1 Generalized Spectral Index Approach

In earlier stage of remote sensing studies, a great deal of effort was spent to devise various spectral indices for applications of satellite and airborne multispectral sensors to classification or quantification of vegetation and other land surfaces. Accordingly, a number of spectral indices have been proposed with specific names such as NDVI, EVI, SAVI, OSAVI, TSAVI, MCARI, and so forth (see Section 2.5). Generally, these indices are calculated using a few waveband data since the normalization of reflectance values by using multiple wavebands is effective in reducing the influence of errors or uncertainty due to atmospheric and background differences, as well as in enhancing and/or linearizing the spectral response to target vegetation (e.g., Huete, 1988; Gitelson et al., 2005; Qi et al., 2012).

However, the wavelengths and bandwidths for those indices are often specific to sensors used in individual studies, and their naming is also arbitrary. This implies that predictive models are also sensor specific and new calibration datasets are always required for each sensor, which would hamper standardization and require extra labor and cost. In addition, such target-oriented naming is insufficient to represent the multiple capability of hyperspectral indices. Alternatively, the generalized spectral index approach using hyperspectral data would allow more precise and flexible application of knowledge on the relationships between hyperspectral data and ecophysiological variables (see Section 2.2). The most typical formulations and expressions of generalized spectral indices are the normalized difference spectral index (NDSI) and ratio spectral index (RSI). Their definitions of the are given by the following equations:

$$\mathrm{NDSI}(x, y) = (y - x)/(x + y) \tag{2.1}$$

where x and y are reflectance (R_i and R_j) or first derivative (D_i and D_j) values at i and j nm over the whole hyperspectral range. For example, the most frequently used vegetation index, Landsat-NDVI, is equivalent to NDSI(R_{660}, R_{830}). Note that R or D should be denoted using the value of the central wavelength in units of nanometers. The derivative processing is effective for enhancing weak spectral features and extracting critical wavelengths by reducing the influence of trends or low-frequency noise (Demetriades-Shah et al., 1990). Similarly, another transformation, RSI, is defined as

$$\mathrm{RSI}(x, y) = x/y \tag{2.2}$$

where both R and D values were also used for x and y.

The contour maps of predictive ability (r^2, RMSE, etc.) for all NDSI or RSI indices using the thorough combinations of two wavebands can provide overview information on the optimal wavebands and bandwidths. The NDSI and RSI formulations are linked to each other but the their response (such as linearity) to a target variable is different. Similar formulations have been employed in many studies to explore useful indices (e.g., Liu et al., 2003; Gitelson and Merzlyak, 1997; Mutanga and Skidmore, 2004; Inoue et al., 2008a,b, 2012b, 2016), but their expressions were not necessarily suitable for standardization, comprehensive comparisons, or wider operational applications.

Additionally, similar approaches can be extended to the various formulations using additional parameters and/or multiple wavebands such as OSAVI (Rondeaux et al. 1996) and TCARI (Daughtry et al. 2000).

$$\mathrm{TCARI} = 3\left[(R_{700} - R_{670}) - 0.2(R_{700} - R_{550})\left(\frac{R_{700}}{R_{670}}\right)\right] \tag{2.3}$$

$$\mathrm{OSAVI} = \frac{(1+0.16)(R_{800} - R_{670})}{(R_{800} + R_{670} + 0.16)} \tag{2.4}$$

The use of nonlinear models (e.g., logarithmic, polynomial) would allow better fitting, and so might result in improvement of predictive ability. Nevertheless, such nonlinear fitting or use of increased number of wavebands usually implies the inclusion of a larger number of model parameters and/or less sensitivity in marginal range of the target variable. Accuracy, robustness, and simplicity have to be balanced depending on sensor systems and applications.

2.3.2 Multivariable Regression Approach

The major advantage of hyperspectra is the large number of wavebands at fine spectral resolution, which are suitable for multivariable statistical analysis as in the laboratory chemometric method (Spiegelman et al., 1998). However, despite the data richness of hyperspectral data, multicollinearity due to the high correlation between wavebands is the inherent problem of multivariable statistical analysis. Multiple linear regression (MLR) is a simple and widely used method in early study stages, but is not suitable for predictive purposes because it is prone to be unstable due to multicollinearity and strongly affected by the number of sample data as well as the number of independent variables (Grossman et al., 1996; Inoue et al., 2008a).

Both principal component regression (PCR) and partial least-squares regression (PLSR) are able to reduce the effects of multicollinearity. The PCR and PLSR methods have similar structures and would be suitable for the analysis of redundant data such as hyperspectra that include a large number of independent variables correlating with each other. Nevertheless, PLSR may be more suitable than PCR for predictive purposes because the principal components in PCR are determined based on the variance of independent variables only, whereas latent variables in PLSR are determined by taking the covariance between the independent and target variables into consideration (Norgaard et al., 2000). PLSR have been used to estimate biochemical variables such as nitrogen content (e.g., Martin et al. 2008). However, according to theoretical and experimental considerations (Spiegelman et al., 1998; Inoue et al., 2008a, 2012b, 2016), the PLSR method may not always provide the best solutions because some of the wavebands are not informative of the target variable or may even disturb useful signatures. Thus, the interval PLSR (iPLSR) may be the most feasible methods for predictive modeling using hyperspectra (Norgaard et al., 2000; Leardi and Norgaard, 2004). In iPLSR, inclusion or exclusion of an individual waveband is determined by its statistical contribution to the root mean squares error (RMSE) in cross validation; that is, an optimal subset of wavebands is explored through the iterative PLSR trials using the thorough subsets of all wavebands so that the RMSE is minimized.

2.3.3 Machine Learning Approach

Machine learning methods such as artificial neural network (ANN) and support vector machine (SVM) would be applied for estimating ecophysiological functioning from hyperspectral data. In general, the ANN consists of interconnected multiple layers for transformation from input data to output data based on optimization of nonlinear models. The SVM is one of the supervised classification algorithms, which constructs a set of kernel feature space of higher dimensionality (hyperplane) for classification of input data by maximizing the distance (margin) between samples. By the introduction of the kernel function, SVM can also be applied to nonlinear problems (Camps-Valls et al., 2006).

These methods require no assumptions on the statistical data distribution and linearity of the relationship between variables (Hansen and Schjoerring 2003; Ali et al. 2015). These approaches have been applied to classification problems using hyperspectral data, but would be applicable to assessment of remote sensing of ecophysiological variables (Del Frate et al. 2003; Durbha et al., 2007; Notarnicola et al., 2008; Ali et al., 2015). They would be useful especially for analysis and/or prediction of biophysical or ecophysiological variables that are influenced by various factors where influences are not formulated explicitly.

However, accuracy and applicability of these predictive models by such data-driven methods are highly dependent on the size and quality of the training datasets (Doktor et al. 2014; Ali et al. 2015). Especially in ecophysiological applications for agricultural and ecosystem problems, acquisition of *in situ* measurements often requires time-consuming, careful, or expensive field work. This would affect the quality and quantity of good training dataset for the application of machine learning methods. In addition, predictive models based on data-driven methods are basically site and sensor specific. Accordingly, we have to be careful about the applicability of such empirical models as well as the accuracy and computational speed (Meroni et al., 2004).

Recent trends in science and technology suggest that these data-driven methods (so-called artificial intelligence, AI) would be powerful tools to solve various problems provided that a large datasets (so-called "big data") are available (Ali et al. 2015). Since the ecophysiological functioning of vegetation is related to many biochemical and photochemical processes, and their relationships are often nonlinear, machine learning methods might provide better predictive ability than statistical and physically based models. It might allow nonexperts to derive moderate predictive models without expertise in a specific field of science. Nevertheless, the necessity of scientific knowledge and expertise should be emphasized in three aspects: (1) optimization of the quantity and quality of training data; (2) appropriate selection of input variables; and (3) evaluation of the soundness and importance of causal relationships or parameterization.

2.3.4 Use of Physically Based Reflectance Models

If a target ecophysiological variable is incorporated explicitly in canopy reflectance models, inversion of such models using hyperspectral measurements may be useful. For example, a physically based reflectance model PROSAIL can simulate the hyperspectral reflectance (1 nm resolution) of a canopy as a function of several ecophysiological variables such as leaf chlorophyll $a + b$ concentration, equivalent water thickness, leaf structural parameter, LAI, and mean leaf inclination angle (LAD: leaf angle distribution) in addition to sun zenith angle and soil reflectance (Jacquemoud et al., 2009;

Bacour et al., 2002). Several approaches such as numerical optimization methods (e.g., Meroni et al., 2004), lookup table approaches (e.g., Combal et al., 2003), and artificial neural networks (e.g., Schlerf and Atzberger, 2006) have been applied for inversion of the model.

The inversion method is attractive because the models describe the underlying mechanisms of canopy reflectance and are basically free from requirements of calibration. However, some inherent or technical constraints such as uncertainty in finding an optimum solution (ill-posed problem), strong need for accurate reflectance, and availability of data for model training or parameterization (e.g., Combal et al., 2003; Darvishzadeh et al., 2008b) may need attention. Nevertheless, physically based models are quite useful for investigating the possible effects of changes in ecophysiological and biophysical status as well as in the measurement configurations to the hyperspectral reflectance of a canopy (Féret et al., 2011). At present, important ecophysiological variables incorporated in physically based models are still limited. It would be useful to incorporate some additional variables such as leaf nitrogen content, light use efficiency and grain protein content as explicit state variables.

2.4 SPECTRAL ASSESSMENT OF PHOTOSYNTHETIC CAPACITY AND EFFICIENCY IN CROPS

The potential photosynthetic capacity in terms of energy is limited by the photosynthetically active radiation (PAR) absorbed by chlorophyll. The close relationship between dry matter production (as NPP) and seasonally integrated APAR was first reported by Shibles and Weber (1966). Accordingly, the use of fAPAR in a simple ecological model (e.g., Monteith, 1977) has been employed in a range of applications for rough assessment of net primary productivity (NPP). In such growth models, leaf area index (LAI) has been used to estimate fAPAR to estimate daily APAR since a close exponential relationship was found in ecological studies (Monsi and Sakei, 1953). Subsequently, due to the inherent close relationship between spectral reflectance (e.g., NDVI) and fAPAR, the APAR in the growth models has been estimated by fAPAR $\times$ PAR directly by using remote sensing data (e.g., Potter et al., 1993; Ruimy et al., 1994; Goetz et al., 1999; Turner et al., 2002). However, the actual productivity is affected by the efficiency in use of APAR in ecophysiological processes (light use efficiency: LUE). LUE is controlled by environmental conditions such as temperature and water and nutrient availability via physiological and photochemical processes (e.g., Peñuelas and Filella, 1998).

$$\mathrm{NPP} = \mathrm{LUE} \times \mathrm{fAPAR} \times \mathrm{PAR} \tag{2.5}$$

This simple model has been used in remote sensing of plant productivity based on semiempirical relationships of spectral indices with fAPAR (capacity) and LUE (efficiency). Accordingly, accurate and robust assessment of these variables is the basis for better understanding and modeling of photosynthetic productivity. Nevertheless, the structure and determinants of both fAPAR and LUE would have to be investigated in more detail in the aspects of ecophysiological and photochemical processes.

2.4.1 PHOTOSYNTHETIC CAPACITY

The fAPAR has been estimated from spectral indices such as NDVI (e.g., Kumar and Monteith, 1982; Asrar et al., 1989; Baret and Guyot, 1991) and applied to production models (e.g., Ruimy et al., 1994; Nouvellon et al., 2000). The relationship is little affected by pixel heterogeneity, LAI, or variation in leaf orientation and optical properties (e.g., Pinter et al., 1985). In fact, the NDVI-fAPAR relationship is rather robust for different crops during the vegetative growth stages (Figure 2.5). However, the relationship is affected by background and bidirectional effects (Myneni and Williams, 1994) and by phenological stages and senescence. The NDVI–fAPAR relationship is largely different between

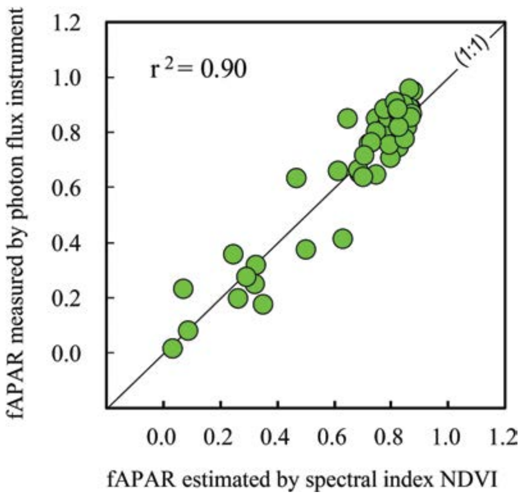

FIGURE 2.5 Comparison of fAPAR (fraction of absorbed photosynthetically active radiation) values estimated by spectral index NDVI and *in situ* measurements during vegetative growth stages in three crops (rice, soybean and corn). (After Inoue, Y. and Olioso, A. 2006. *Journal of Geophysical Research*, 111(D24), D24S91, doi:10.1029/2006JD007469.)

before and after heading (anthesis) in most crops (e.g., Daughtry et al., 1983; Asrar et al., 1989; Inoue and Iwasaki, 1991; Inoue et al., 1998; Choudhury, 2000).

An analysis by Inoue et al. (2008b) clearly showed the limitation of NDVI based on generalized spectral index approach using hyperspectral data and *in situ* fAPAR measurements during the entire growth season (Figure 2.6). According to the NDSI-map, that is, a contour map of predictive ability, the NDVI with Landsat bands was not the best predictor of fAPAR due to the distinct difference before and after the heading stage. Alternatively, the NDSI(R_{720}, R_{420}) had the high and consistent predictive ability throughout entire growth stages. This analysis was based on a dataset for rice, but the results would be common to the other crops in Figure 2.5.

Note that the total photosynthetically active radiation absorbed by a plant canopy (APARt) is the maximum energy source for photosynthesis used in the simple growth models (e.g., Monteith, 1977). However, the APARt is not always used fully for photosynthesis because of the absorption by nonphotosynthetic or senescent plant elements. Accordingly, the assessment of fAPARc, that is, the part of APARt absorbed by chlorophyll and used for photosynthesis (APARc) should be another important target of remote sensing. In other words, the traditional LUE represents an overall efficiency that integrates the biophysical efficiency in photon absorption by a canopy and the photochemical efficiency (LUEc) in use of absorbed photons. Separate estimation of fAPARc and LUEc would be more suitable to assess the dynamic change of photosynthetic activity of a canopy.

Another variable related to the photosynthetic capacity is P_{max} which represents the maximum photosynthetic rate at the saturating APAR. P_{max} was found to be moderately correlated with RVI using red and near-infrared bands, GRI (green ratio index) using green and red ands, and MSAVI (modified soil adjusted vegetation index; Qi et al., 1994), and four new indices, NDSI(R_{518}, R_{676}), NDSI(R_{620}, R_{623}), NDSI(R_{620}, R_{637}), and NDSI(R_{750}, R_{761}) ($r^2 = 0.65$–0.66). In principle, P_{max} may not be highly correlated with actual P_n since P_{max} is the potential photosynthesis at the highest incident radiation without any stresses. Nevertheless, it is interesting that these wavelengths are all within the wavelength region of chlorophyll *a* and *b* absorption. These results suggest that conventional indices using red and near-infrared wavelength regions (e.g., RVI, GRI, and MSAVI) could be useful for a rough assessment of P_{max}.

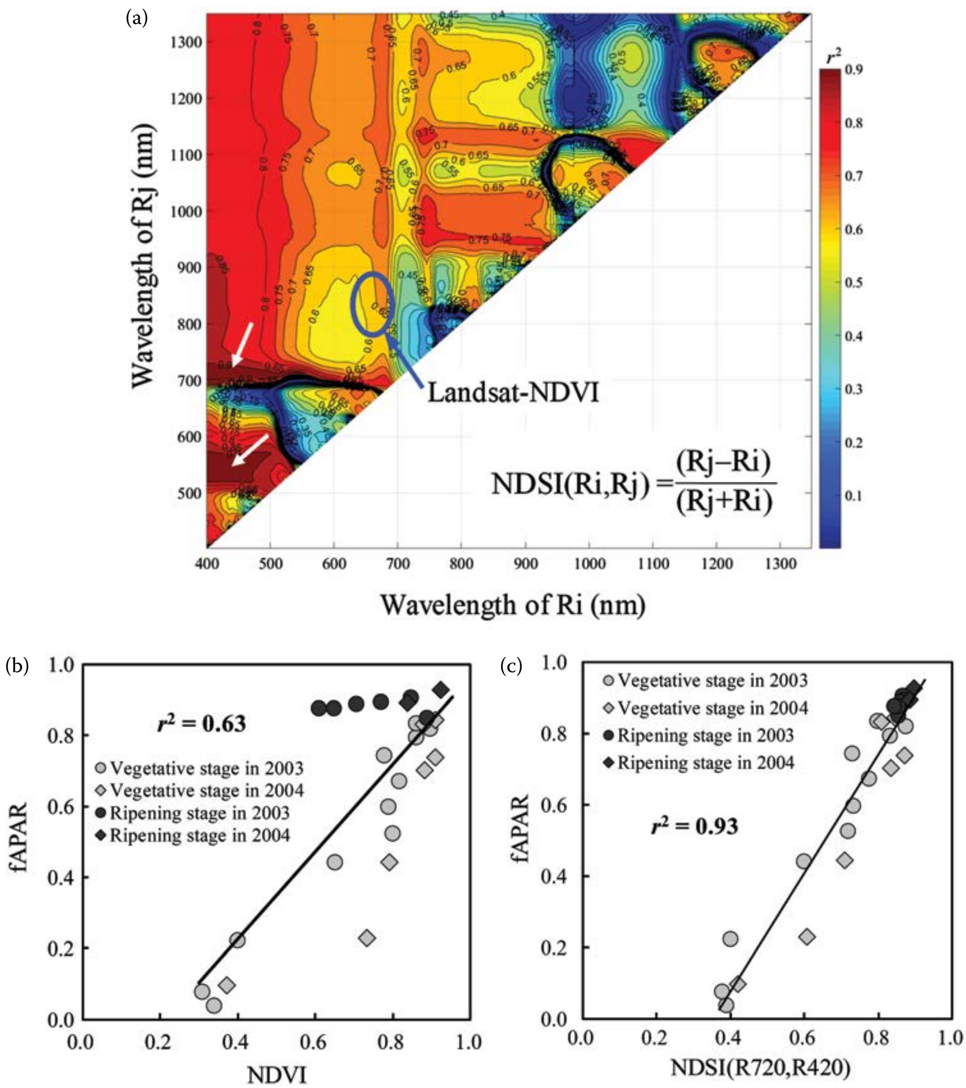

FIGURE 2.6 NDSI map of predictive ability for fAPAR in rice canopies (a) and relationships of spectral indices with the *in situ* measurements of fAPAR with (b) NDVI and (c) NDSI(R_{720}, R_{420}). The white arrows indicate the most significant spots. (After Inoue, Y. et al., 2008b. *Remote Sensing of Environment*, 112, 156–172.)

2.4.2 Photosynthetic Efficiency

The light use efficiency LUE may be assumed to be constant under nonstressed conditions, but it is affected by phenological stages and by abiotic or biotic stresses via ecophysiological processes (e.g., Kiniry et al., 1989; Sinclair, 1994; Peñuelas and Filella, 1998; Choudhury, 2000). Hence, it would be inappropriate to assume constant LUE, especially for assessment of canopy carbon exchange at short temporal resolution (e.g., daily or shorter).

The photochemical reflectance index PRI has been found to be closely related to photosynthetic radiation use efficiency of plant leaves (Gamon et al., 1992; Peñuelas et al., 1995).

$$\mathrm{PRI} = (R_{531} - R_{570})/(R_{531} + R_{570}) \tag{2.6}$$

The relationship can be explained based on the photochemical reactions (see Section 2.2), and has been investigated in a wide range of vegetation, sensors, and scales (Garbulsky et al., 2010). Investigated vegetations ranged from uniform crops to heterogenous forest, and sensors also ranged from ground-based or airborne hyperspectral sensors (e.g., ASD, CASI, AVIRIS) to coarse satellite sensors (e.g., MODIS). The LUE or related ecophysiological variables were measured by photosynthetic instruments (IRGA, PAM) for leaves, estimated directly by eddy covariance methods (flux tower) for ecosystems, or estimated indirectly from the other measurements for larger scales. The available evidence indicates that the PRI may be a useful indicator of ecophysiological variables closely related to the photosynthetic efficiency at the leaf and canopy levels over a wide range of species (Garbulsky et al., 2010). However, a consistent and robust PRI–LUE relationship is not established for several reasons, such as uncertainty of *in situ* measurements of LUE and/or various confounding factors (Garbulsky et al., 2010). Apparent close relationships obtained for broadband and coarse spatial resolution sensors might be indirect and attributable to the linkage of LUE with other biophysical variables. Accordingly, the generalized application of PRI, especially to satellite sensors, may be questionable. At least, hyperspectral or narrow-band reflectance data as well as the reliable *in situ* measurement of LUE would be needed for precise analysis of PRI–LUE relationships.

Generally, actual LUE values have been estimated by photosynthetic instruments for leaves or by EC (eddy covariance) method for ecosystems. Nevertheless, the spatial representativeness of LUE for the vegetated area is a difficult issue especially in heterogeneous ecosystems. Moreover, the matching of image pixels and footprint of EC is critical for precise analysis, especially in the analysis of satellite images. Thus, precise datasets of hyperspectral data and concurrent LUE data for a uniform crop vegetation with fewer confounding factors would be useful to create definitive evidence for remote sensing of photosynthetic efficiency. Here, the applicability of PRI and other potential spectral indicators for remote sensing of LUE are discussed based on the studies on crops.

2.4.2.1 Leaf Scale Assessment Based on Hyperspectral and Photosynthetic Measurements

Light use efficiency or photosynthetic parameters may be accurately determined by the light (PPFD: photosynthetically active photon flux density) vs. net photosynthesis (P_n μmolCO_2 m^{-2} s^{-1}) curve, which is expressed by the following equation:

$$P_n = P_s(1 - \exp[-\varphi \cdot \text{PPFD}]) - R \tag{2.7}$$

where P_n is the net photosynthetic rate; P_s is the saturated photosynthetic rate; φ is the quantum use efficiency; and R is the dark respiration. LUE (μmolCO_2 μmolPhotons^{-1}) is calculated as the ratio of P_n to PPFD. Figure 2.7 shows some examples of PPFD–P_n curves for soybean leaves (*Glycine max* L. Merr.) and concurrent reflectance spectra of leaves under a wide range of PPFD, leaf chlorophyll index (CI), and soil water content (θ) (Inoue and Peñuelas, 2006). This dataset allowed analysis of the relationships of photosynthetic parameters (P_n, P_s, φ, and LUE) with spectral indices (e.g., NDVI, WI, GRI, SIPI, NPQI, SWWI, and WI/NDVI), where the water index was WI = R_{900}/R_{970}, green ratio index GRI = R_{830}/R_{550}, structural independent pigment index SIPI = $(R_{800} - R_{445})/(R_{800} + R_{680})$, normalized phaeophytinization index NPQI = $(R_{415} - R_{435})/(R_{415} + R_{435})$, shortwave infrared water index SWWI = R_{800}/R_{1650}, and WI/NDVI (Inoue et al., 1993; Peñuelas and Filella, 1998; Peñuelas and Inoue, 1999). These spectral indices were assumed to have close or moderate correlations with photosynthetic parameters, but detailed correlation analysis among all variables revealed that PRI–LUE was the only highly significant relationship for inferring the photochemical status directly from the reflectance spectra (Figure 2.8). The PRI–LUE relationship was significantly close under each level of soil water contents, although its slope was strongly affected by soil moisture (water stress). In this case, a consistent PRI–LUE relationship under changing soil water conditions was derived successfully by normalizing the influence of soil water content on the PRI–LUE relationship. Contrarily, chlorophyll concentration had no significant effect on LUE as well as the PRI–LUE

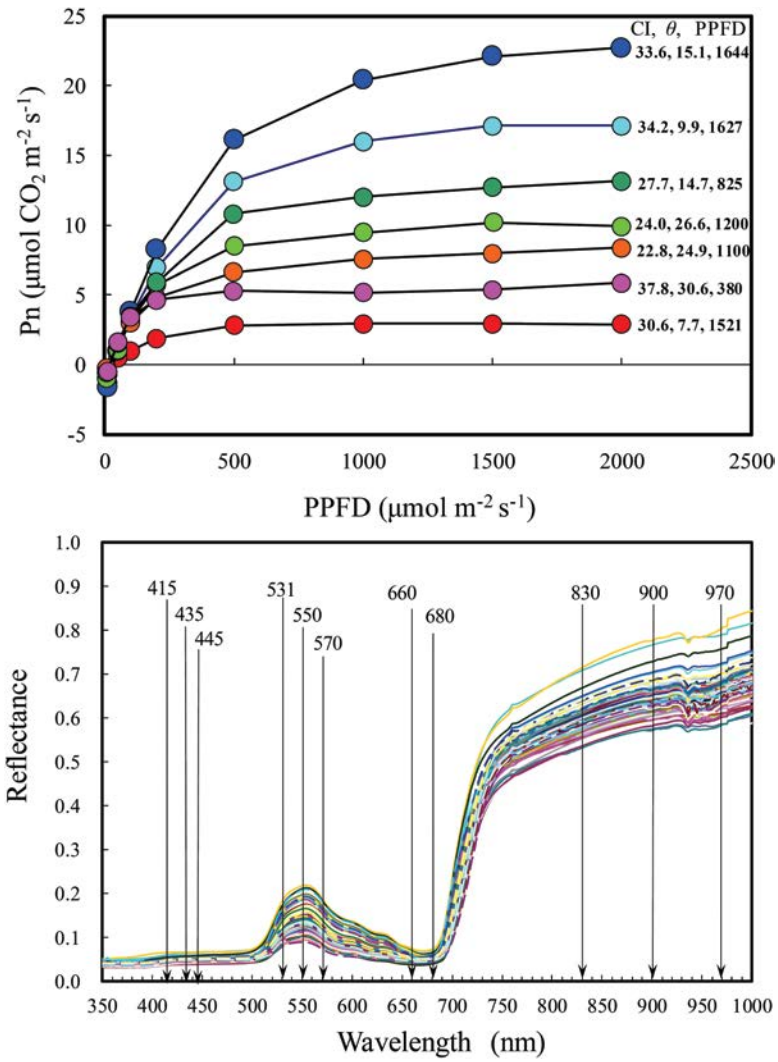

FIGURE 2.7 Light–photosynthesis curves of soybean leaves with different chlorophyll content (CI), soil water content (θ), and photosynthetically active radiation (PPFD) (upper), and spectral reflectance of the leaves (lower). The arrows labeled with wavelength are main spectral wavebands selected based on previous studies on spectral characteristics of plant leaves. Each curve indicates the average of 10 repeated measurements (After Inoue, Y. and Peñuelas, J. 2006. *International Journal of Remote Sensing*, 27, 5249–5254.)

relationship, while the range of CI was large. This may be because both LUE and PRI indicate the photosynthetic functioning of chloroplasts, although the CI simply indicates the density of chloroplast per unit leaf area. These results suggest that PRI would be able to detect relatively rapid photochemical changes caused by PPFD changes, whereas the effects of slower changes such as those in soil water content and chlorophyll content would have to be incorporated differently in predictive modeling (Inoue and Peñuelas, 2006).

The radiation use efficiency (RUE gDM MJ^{-1}) is usually defined as the ratio of dry matter increment to the integrated APAR for a day or longer term (Shibles and Weber, 1966). Accordingly, RUE is more robust and representative of plant productivity at a canopy scale than is LUE (μmolCO_2 μmolPhotons^{-1}) which is a dynamic measure of photosynthetic functioning at leaf scale. It would be

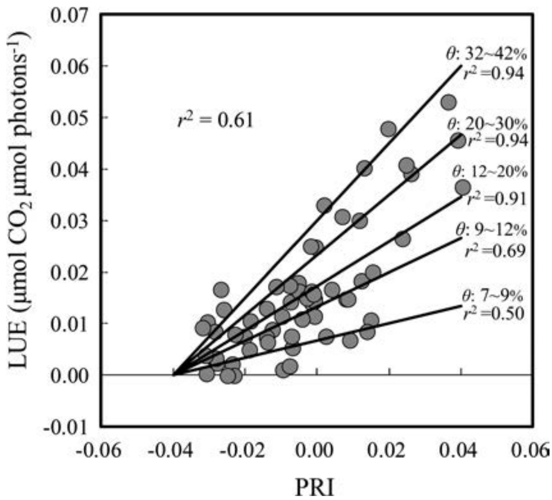

FIGURE 2.8 Relationship between light use efficiency (LUE) and photochemical reflectance index (PRI) as affected by soil water content θ. Regression lines were determined for data points grouped by soil water content; 7%–9%, 9%–12%, 12%–20%, 20%–30%, 32%–42%. (After Inoue, Y. and Peñuelas, J. 2006. *International Journal of Remote Sensing*, 27, 5249–5254.)

reasonable to utilize the LUE as an indicator for leaf-scale diagnosis of photosynthetic functioning, whereas RUE would be suitable for assessment of integrated efficiency at a day or longer temporal resolutions. Scaling from leaf to canopy is an important but difficult issue especially for this type of narrow-band indices due to various confounding factors (Barton and North, 2001). Therefore, both temporal and spatial resolutions have to be carefully considered for spectral assessment of LUE and RUE.

2.4.2.2 Canopy Scale Assessment Based on Hyperspectral and Eddy Covariance Measurements

During the past decade, LUE values estimated from the CO_2 flux and environmental data at flux towers have been used for the analysis of the PRI–LUE relationship (Garbulsky et al., 2010). However, most flux towers were installed in natural or seminatural ecosystems such as grassland, rangeland, and forest, where the spatial and species heterogeneity is large. In addition, it is difficult to acquire precise *in situ* hyperspectral reflectance data in such ecosystems. Therefore, seasonal datasets of the precise measurements of hyperspectral reflectance data and flux data acquired in uniform crop ecosystems such as rice fields would be useful for detailed ecophysiological and remote sensing analysis. The experimental study by Inoue et al. (2008b) may be the first such analysis.

In their analysis, the CO_2 flux data at intervals of 30 min and micrometeorological data as well as the hyperspectral reflectance data for the entire growth stages were used (Figures 2.9 and 2.10). The net ecosystem exchange of CO_2 (NEE_{CO2}) was low for several weeks after transplantation, but CO_2 uptake at midday became obvious even at the low LAI. The midday peak value of NEE_{CO2} increased with increasing LAI and decreased rapidly during the late ripening period. The photosynthetic rate was much lower during the ripening stage than during the early vegetative stage, with similar or larger values of green LAI. Generally, the combination of a footprint model (Kljun et al., 2004) with micrometeorological data and remotely sensed images is useful to confirm the spatial representativeness of the flux data for the ecosystem (Inoue and Olioso, 2006).

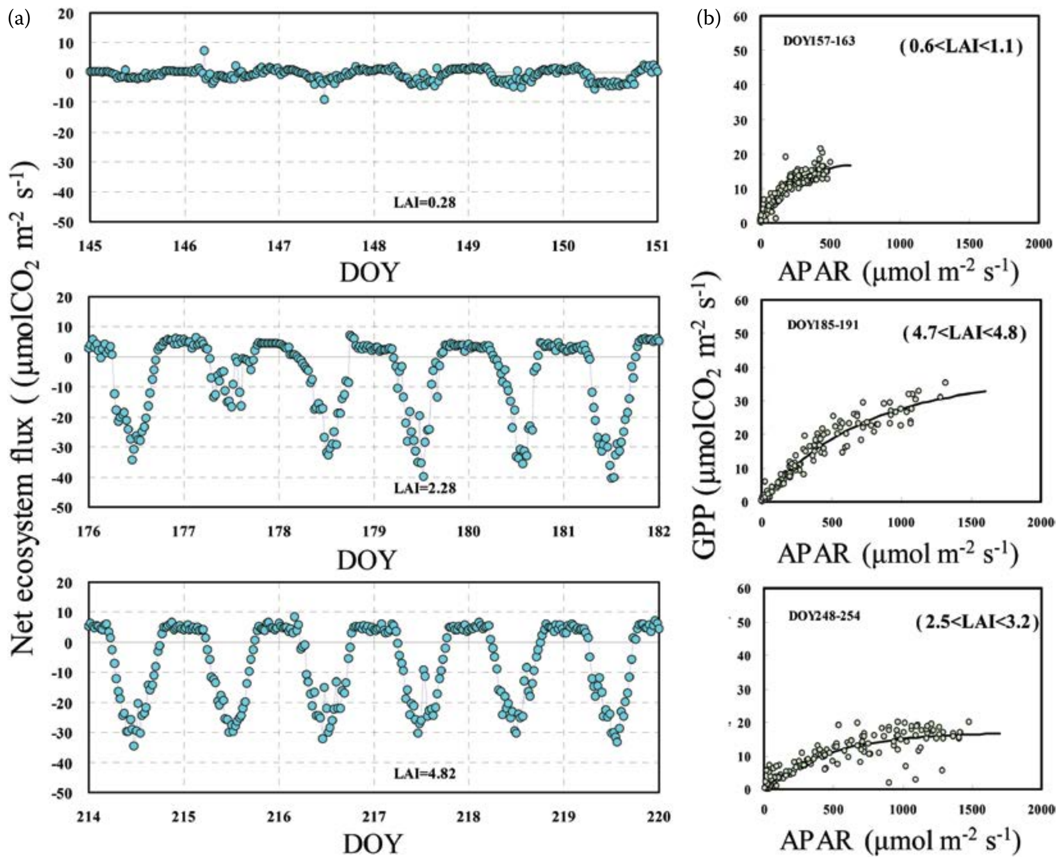

FIGURE 2.9 Seasonal change of net ecosystem CO_2 exchange (NEE_{CO2}) in a rice field measured by eddy covariance method (a), and APAR–GPP relationship (b) during early (upper), middle (middle), and late (lower) growth stages. (After Inoue, Y. et al., 2008b. *Remote Sensing of Environment*, 112, 156–172.)

Photosynthetic efficiency parameters can be determined from these datasets by using the asymptotic exponential equation as follows:

$$GPP = P_{max}\,(1 - \exp[-\varphi \cdot APAR/P_{max}]) \tag{2.8}$$

where GPP is the gross primary productivity, φ is the initial slope of the curve (quantum efficiency), and P_{max} is the maximum photosynthetic rate at the saturating APAR (Figure 2.9b). Two indicators of canopy light use efficiency at the time of remote sensing measurements were estimated from half-hourly data of CO_2 and photon flux data.

$$LUE_N = NEE_{CO2}/APAR \tag{2.9}$$

$$LUE_G = GPP/APAR \tag{2.10}$$

The generalized spectral index approach was applied to explore new spectral indices and to evaluate the predictive ability of previous indices. Figure 2.11 shows the NDSI map of predictive ability of thorough combination of two wavebands for assessment of LUE_G. The map can provide an overview of the statistical significance of all NDSIs for selecting the optimal central wavelength and bandwidth. There are several narrow peaks (reddish) and deep troughs (bluish). Some steep walls

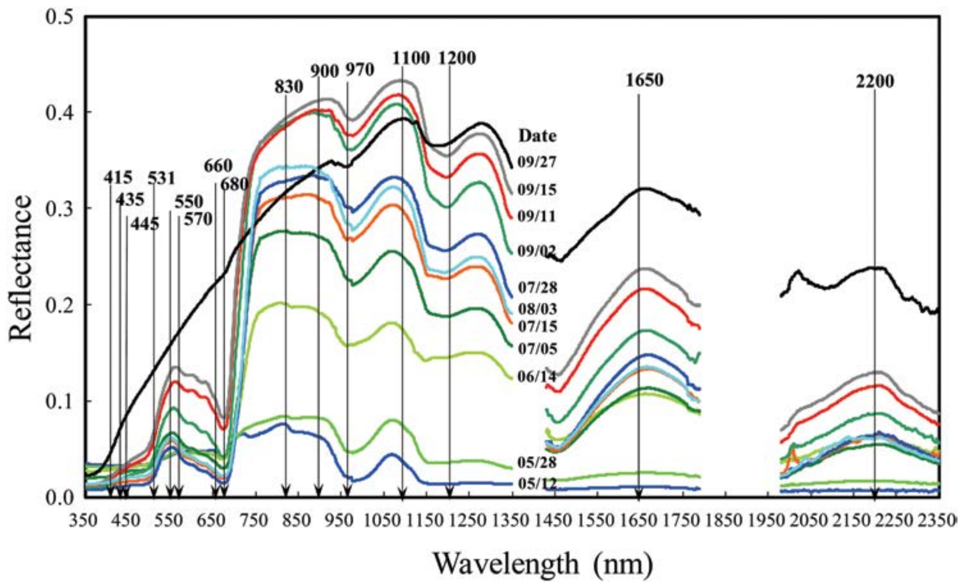

FIGURE 2.10 Seasonal change of reflectance spectra in a rice canopy associated with the growth shown in Figure 2.8. Date numbers indicate month/day. Wavelengths indicated with arrows were used to derive conventional spectral indices. (After Inoue, Y. et al., 2008b. *Remote Sensing of Environment*, 112, 156–172.)

are also found (e.g., around the 530 vs. 560 nm region). Therefore, selection of effective wavelengths should be made carefully so as not to span such steep-wall regions, since even a small bias could largely reduce the potential significance.

The LUE_G was best correlated with NDSI(R_{710}, R_{410}), NDSI(R_{710}, R_{520}), and NDSI(R_{530}, R_{550}) derived from nadir measurements, while most conventional indices were less well correlated. R_{550}, R_{710}, and R_{1122} were selected for multiple indices presumably because they have some specific role in ecophysiological processes that directly or indirectly affect photosynthetic efficiency at a canopy scale. R_{710} is positioned around the red-edge wavelengths, which represent the amount of chlorophyll. Therefore, R_{710} may have a role in normalizing the amount of vegetation when it is used with other visible wavelengths such as 410 or 530 nm. The performance of PRI was surprisingly poor in this analysis, but R_{530} may have significant role in detection of photosynthetic rate because NDSI(R_{530}, R_{550}) was highly correlated with LUE_G. The use of R_{550} nm instead of R_{570} nm in PRI as a reference wavelength may significantly improve the estimation of photosynthetic efficiency. R_{1122} may be related to the amount of canopy nitrogen because 1120 nm is the wavelength of lignin absorption (Curran, 1989), and lignin/cellulose content is inversely related to nitrogen content during the growing season.

The quantum efficiency φ was best correlated with NDSI(R_{450}, R_{1330}). It is interesting that NDSI(R_{403}, R_{830}) and NDSI(R_{420}, R_{970}) using very far wavelengths were also highly correlated with φ, whereas some other NDSIs use nearby wavelengths such as NDSI(R_{933}, R_{940}), NDSI(R_{933}, R_{948}), and NDSI(R_{1053}, R_{1058}). The bandwidth is relatively broad for the former NDSIs (5–80 nm) and narrow for the latter NDSIs (3 nm). The WI using R_{970}, a weak absorption peak of water, proved useful for detecting leaf water status (Peñuelas and Inoue, 1999). This may explain the high correlations of WI with φ and LUE_G, since the leaf water status strongly affects photosynthetic efficiency. Although no previous literature suggested the role of the 930–950 nm region, it may have potential for estimating φ.

The results described were obtained using nadir spectral data, but off-nadir measurements would have additional potential since the photosynthetic efficiency is related the photochemical processes or photosynthetic rate per unit leaf area and oblique reflectance measurement would allow acquisition

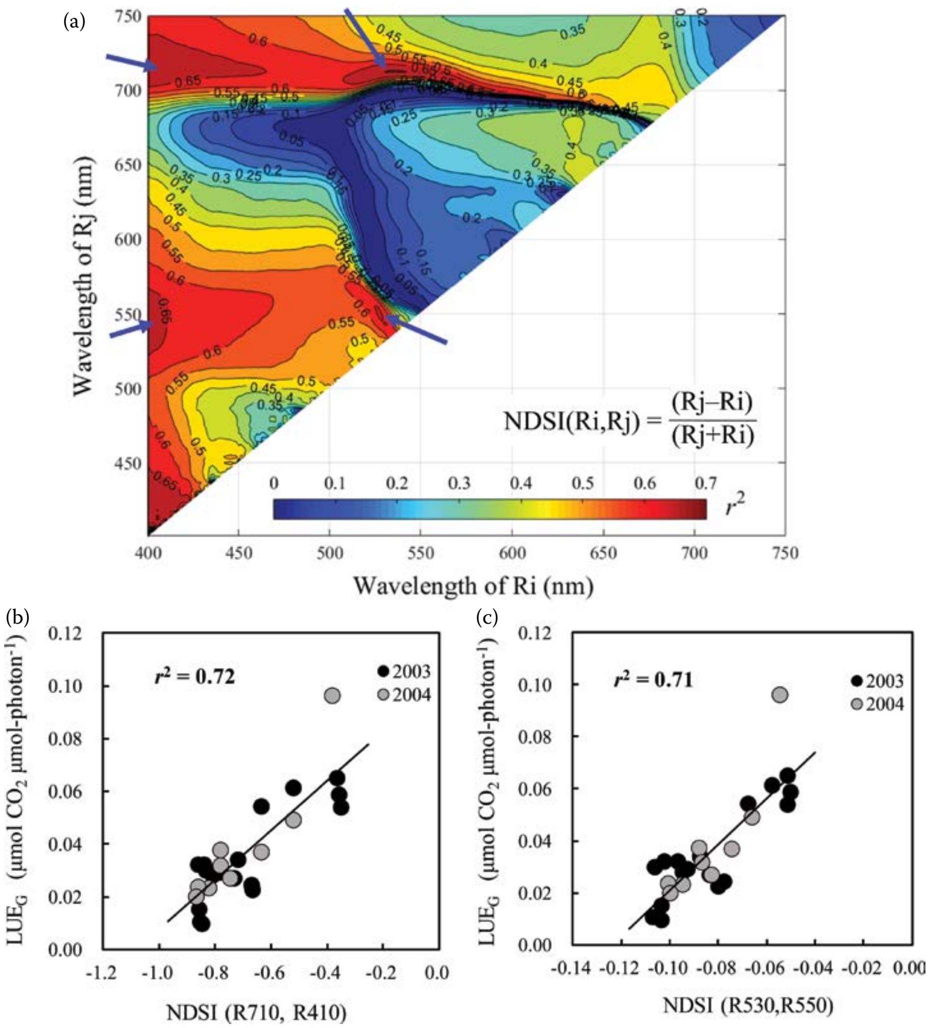

FIGURE 2.11 NDSI map of predictive ability for LUE_G in rice canopies (a) and relationships of promising spectral indices with the LUE_G (b,c). The arrows in the NDSI map indicate most significant positions. (After Inoue, Y. et al., 2008b. *Remote Sensing of Environment*, 112, 156–172.)

of spectral data of leaves only. Recent advances in drone (unmanned aerial vehicle: UAV) platforms enable flexible measuring configurations including off-nadir observation (Verhoeven, 2011; Roosjen et al., 2017). The analysis using off-nadir measurements suggested promising capability of new spectral indices for assessment of LUE_G or LUE_N (Figure 2.12). Overall, off-nadir measurements were more closely related to the efficiency parameters than nadir measurements. Figure 2.12 suggested the region consisting of 400–440 nm vs. 400–500 nm had rather high predictive ability, while there is a deep trough around the 410–530 nm vs. 500–580 nm region. It is interesting that the 400–420 nm regions showed a high correlation ridge along R_{422}. Figure 2.13 shows a close-up view of two significant parts in the contour map of r^2 between φ and NDSIs derived from off-nadir measurements. A ridge of high r^2 was found along 413 nm, while the other regions showed poor correlations. It is noteworthy that R_{435} included in the NQPI proved to be significant in assessment of LUE. In contrast, relatively large regions had high r^2 values around the 1000–1120 nm vs. 1100–1130 nm and the 1130–1150 nm vs. 1160–1200 nm regions (Figure 2.13b).

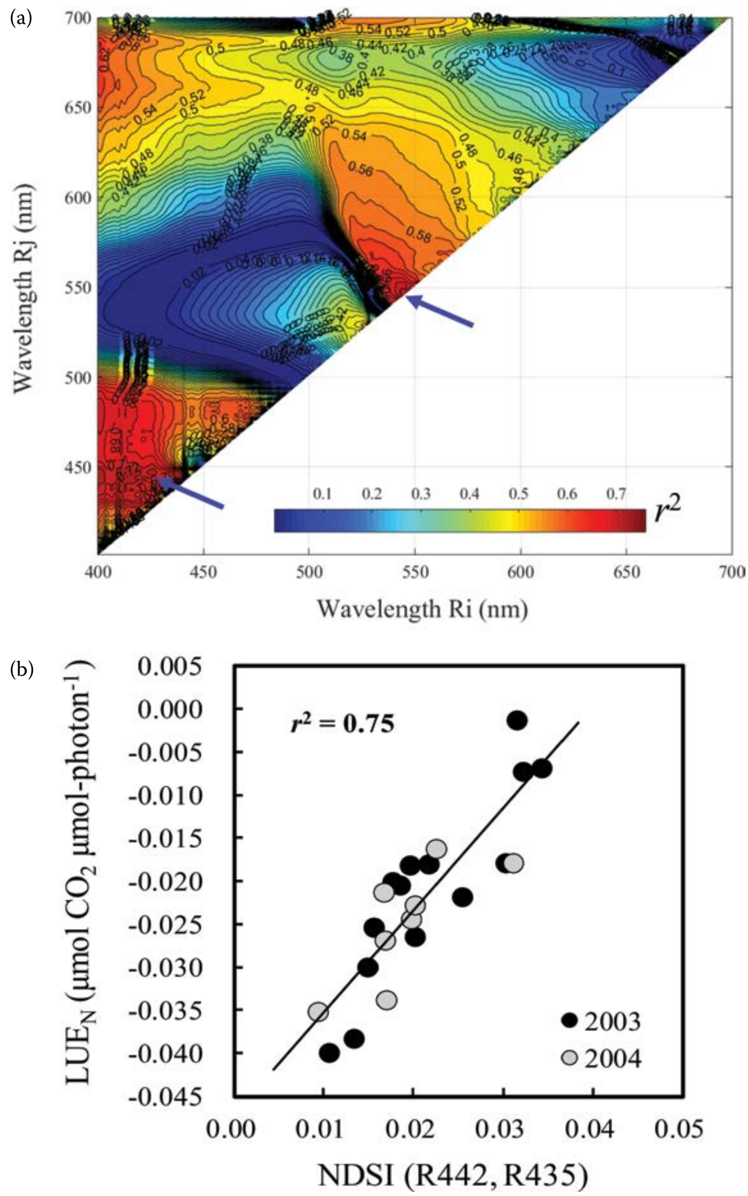

FIGURE 2.12 NDSI map of predictive ability for LUE$_N$ in rice canopies (a) and relationships of promising spectral indices with the LUE$_N$ (b). The arrows in the NDSI map indicate most significant positions. This result was derived from off-nadir observations. (After Inoue, Y. et al., 2008b. *Remote Sensing of Environment*, 112, 156–172.)

These experimental results would provide useful insights for the assessment of radiation use efficiency and photosynthetic capacity in other ecosystems. Nevertheless, the underlying ecophysiological mechanisms for the predictive ability of spectral indices are not well identified at the moment, except for the well-known absorption features of major pigments and materials such as chlorophyll, xanthophyll, carotenoids, and water (Gamon et al., 1992; Inoue et al., 1993; Peñuelas and Filella, 1998, Daughtry et al., 2000). Further studies are needed to examine their applicability to wider range of ecosystems and to investigate the ecophysiological and photochemical mechanisms to systematically account for the effects of biotic and abiotic stresses.

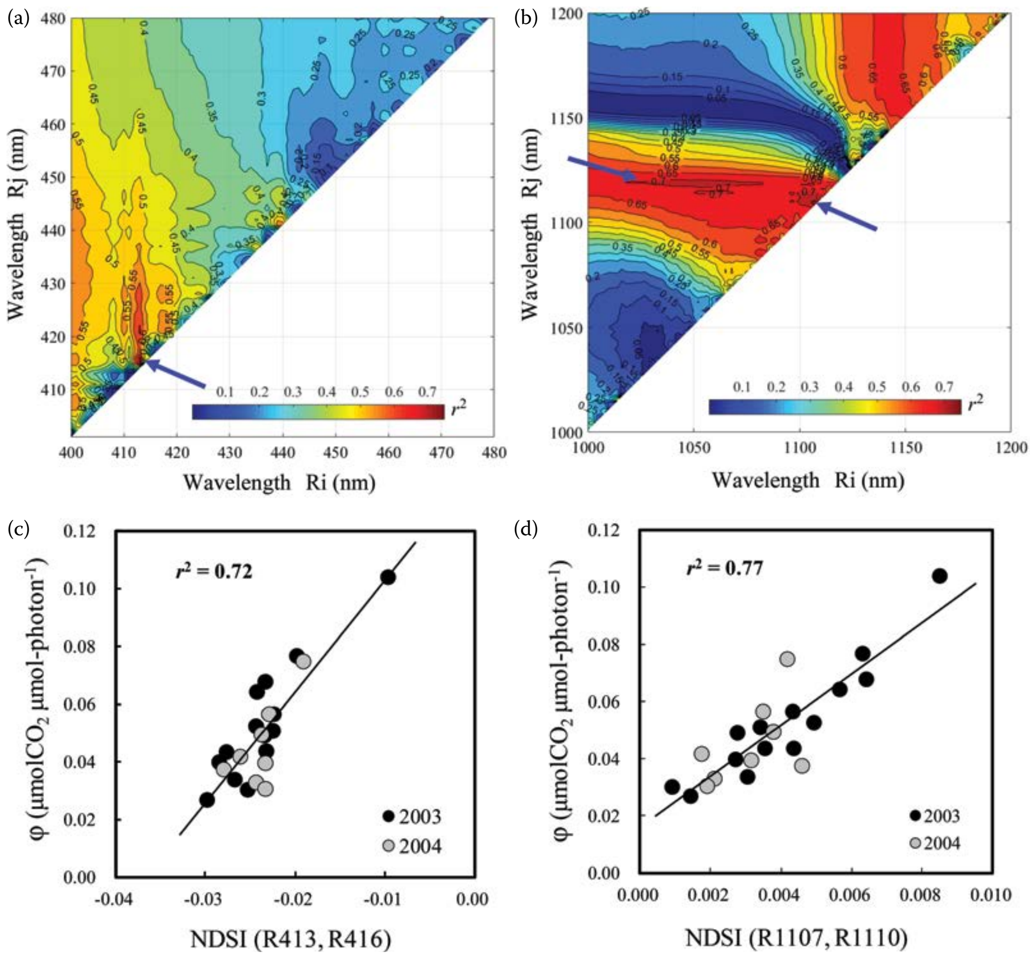

FIGURE 2.13 NDSI maps of predictive ability for quantum efficiency (φ) in rice canopies (a,b) and relationships of promising spectral indices with the φ (c,d). The arrows in NDSI-maps indicate most significant positions. These results were derived from off-nadir observations. (After Inoue, Y. et al., 2008b. *Remote Sensing of Environment*, 112, 156–172.)

2.5 SPECTRAL ASSESSMENT OF DIAGNOSTIC INFORMATION FOR CROP MANAGEMENT

2.5.1 Chlorophyll Content for Growth Monitoring

The canopy-scale photosynthetic capacity is determined to a large extent by the absorptivity of PAR by chlorophyll (fAPARc). The fAPARc is determined by the density and spatial distribution of chlorophyll pigments within the canopy. The 3D distribution of chlorophyll within a canopy is often expressed by using the area of green leaves (LAI), leaf chlorophyll content (LCC) and leaf angle distribution (LAD). In a wide range of canopy photosynthetic models, the potential photosynthetic rate per leaf area (P_n) is used with LAI and LAD to express the 3D distribution of photosynthesis (De Pury and Farquhar, 1997; Roy et al., 2001). In simple models, the LAI has been used to represent the photosynthetic capacity of a canopy with a constant value of LUE by assuming that the effects of variability in LCC, LAD, and clumping are negligible (Monteith, 1977; De Pury and Farquhar, 1997; Choudhury, 2000). However, determination of green LAI is not simple or is rather arbitrary because the green and nongreen threshold is unclear. In addition, the potential P_n is strongly controlled by the chlorophyll ($a + b$) concentration per unit leaf area LCC (Nobel, 2005). Accordingly, the amount of chlorophyll content per unit land surface (CCC) is the major determinant of the fAPARc although the spatial distribution of chlorophyll would affect the light absorption to some extent (Pinter et al., 1985; Jacquemoud et al., 2009). Thus, accurate determination of the total CCC would be the most essential and robust basis for ecophysiological modeling.

On the other hand, the chlorophyll content or greenness of crop leaves has been used as a diagnostic indicator for fertilizer management owing to the close relationship between nitrogen and chlorophyll contents in green leaves (Houlès et al., 2007; Inoue et al., 2012b). In rice leaves, for example, 75%–85% of the total nitrogen is included in chloroplast throughout the growing period although a part of nitrogen is allocated into nongreen parts such as grain (Morita, 1978).

Therefore, the accurate and timely assessment of ecosystem CCC by remote sensing is vital for a wide range of agricultural and ecological applications such as diagnostics for crop management, assessment of degradation/exuberance of terrestrial vegetation, and monitoring of ecosystem carbon balance. This is why chlorophyll has been one of the major targets of optical remote sensing (e.g., Vogelmann et al., 1993; Blackburn, 1998; Daughtry et al., 2000; Dash and Curran, 2004; Gitelson et al., 2005). A number of spectral indices have been proposed specifically for assessment of chlorophyll content in leaf or canopy scales (e.g., Inada, 1985; Shibayama and Akiyama, 1986; Daughtry et al., 2000; Broge and Leblanc, 2000; Richardson et al., 2002; Dash and Curran, 2004; Gitelson et al., 2005; Delegido et al., 2008). The pioneering study by Inada (1985) was used as a basis for the handheld chlorophyll meter SPAD-502 (Minolta). The critical role of the red edge wavelength region for leaf and canopy chlorophyll status has been recognized by many studies (e.g., Vogelmann et al., 1993; Gitelson et al., 2005). However, comparative studies on accuracy and robustness of various methods using diverse hyperspectral data and in situ measurements are still very few (Martin et al. 2008, Inoue et al., 2016).

The study by Inoue et al. (2016) made a comprehensive comparison of generalized spectral index approach (NDSIs and RSIs) and multivariable regression approach (PLSR and iPLSR) for assessment of CCC using diverse hyperspectral datasets taken in different locations and species. Their comprehensive study revealed the relative advantages and disadvantages of the majority of spectral models in the aspects of accuracy, linearity, robustness, simplicity, and versatility (Figure 2.14).

Overall, previous indices proposed for CCC using red edge and green wavebands, such as VOG-3, GMI-2, $CI_{red\text{-}edge}$, CI_{green}, and MTCI, proved to have moderate to excellent predictive ability. Nevertheless, an SI-based model using RSI(R_{815}, R_{704}), that is, the ratio of reflectance values at 815 and 704 nm, was found to be superior to all other models in overall predictive ability of CCC (Figures 2.14 and 2.15). The λ_{rep} model using the red edge position proved to have a limitation because actual wavelength shift might be beyond the range assumed by the model. Generally, spectral models proposed for leaf-scale variables (e.g., MCARI, PRI, SIPI) did not show good predictive ability for assessment of CCC as suggested in preceding studies (le Maire et al. 2008).

It is interesting that PLSR and iPLSR models using much larger number of wavebands proved to be inferior to the index-based models, especially in versatility. This may be attributable to the over-fitting to the calibration dataset. Their performance was poor, especially in different plant types (Figure 2.15). Multivariable regression methods (e.g., PLSR) and machine learning methods (e.g., support vector machine and artificial neural network) can be applied to hyperspectral data (Hansen and Schjoerring, 2003; Ali et al., 2015). However, the applicability of multivariable regression models to different sensors and/or different types of vegetation proved unstable. Accuracy and applicability of data-driven models by machine learning methods are highly dependent on the size and quality of the training datasets (Doktor et al., 2014; Ali et al., 2015).

The soundness of the SI-based models was inferred by simulation results using a physically based reflectance model (PROSAIL) under various canopy conditions including plant types (canopy geometry), LCC, LAI, and soil background (Figure 2.16). The generalized SI approach has unique advantages in simplicity, interpretability, robustness, and applicability compared to these methods. Additionally, the SI contour map approach using hyperspectral data can provide clear overview for

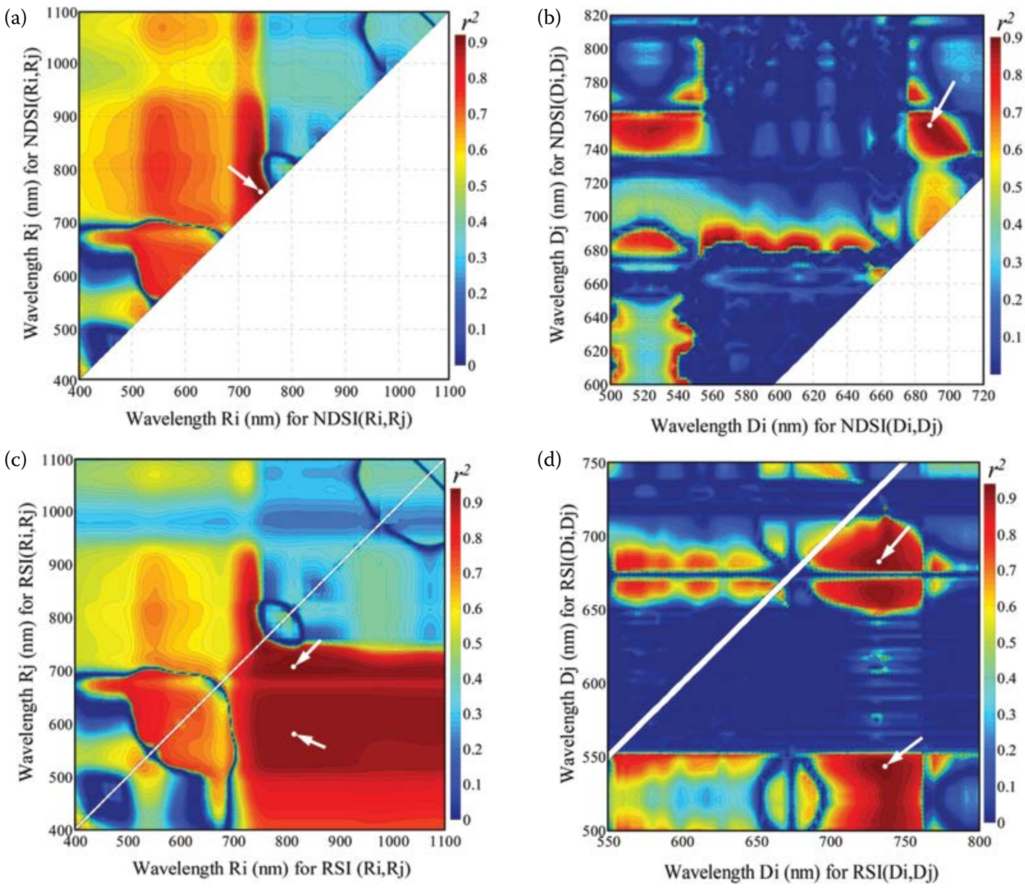

FIGURE 2.14 NDSI and RSI maps of predictive ability for canopy chlorophyll content (CCC) in rice canopies using reflectance spectra (a,c) and first derivative spectra (b,d). The white arrows indicate the most significant spots. (After Inoue, Y. et al., 2016. *Plant, Cell and Environment*, 39, 2609–2623.)

selecting optimal wavebands and bandwidths for various sensors. The best RSI model would be used as a simple and robust algorithm for the canopy-scale chlorophyll meter and/or remote sensing of CCC in ecosystem and regional scales. The model is now applied to the diagnostics for fertilizer management in rice and wheat using both satellite and drone-based image data (Inoue, 2017; Inoue and Yokoyama, 2017).

2.5.2 Nitrogen Content for Fertilizer Management

Nitrogen is essential for higher photosynthetic functioning and productivity in plants. The significant increase in crop yield over the past century is nearly proportional to the increase in nitrogen fertilizer applied to farmland (e.g., Dobermann and Cassman, 2004; Nishio, 2005). However, nitrogen fertilizer is also a significant nonpoint source of water and atmospheric pollution. Groundwater contamination with nitrate nitrogen (NO_3-N) is a serious problem in many countries (e.g., MAFF-UK, 2000; Nishio, 2005; Inoue et al., 2012a). Furthermore, Ishijima et al. (2007) demonstrated that nitrogen fertilizer is an important source of nitrous oxide (N_2O) in the atmosphere.

Therefore, agricultural management practices should aim for efficient use of nitrogen to achieve high-yielding and high-quality crop production with minimal environmental impacts. Site-specific farm management, that is, precision agriculture based on remote sensing, is a promising approach to attaining such intelligent crop management practices (e.g., Moran et al., 1997; Inoue, 2003;

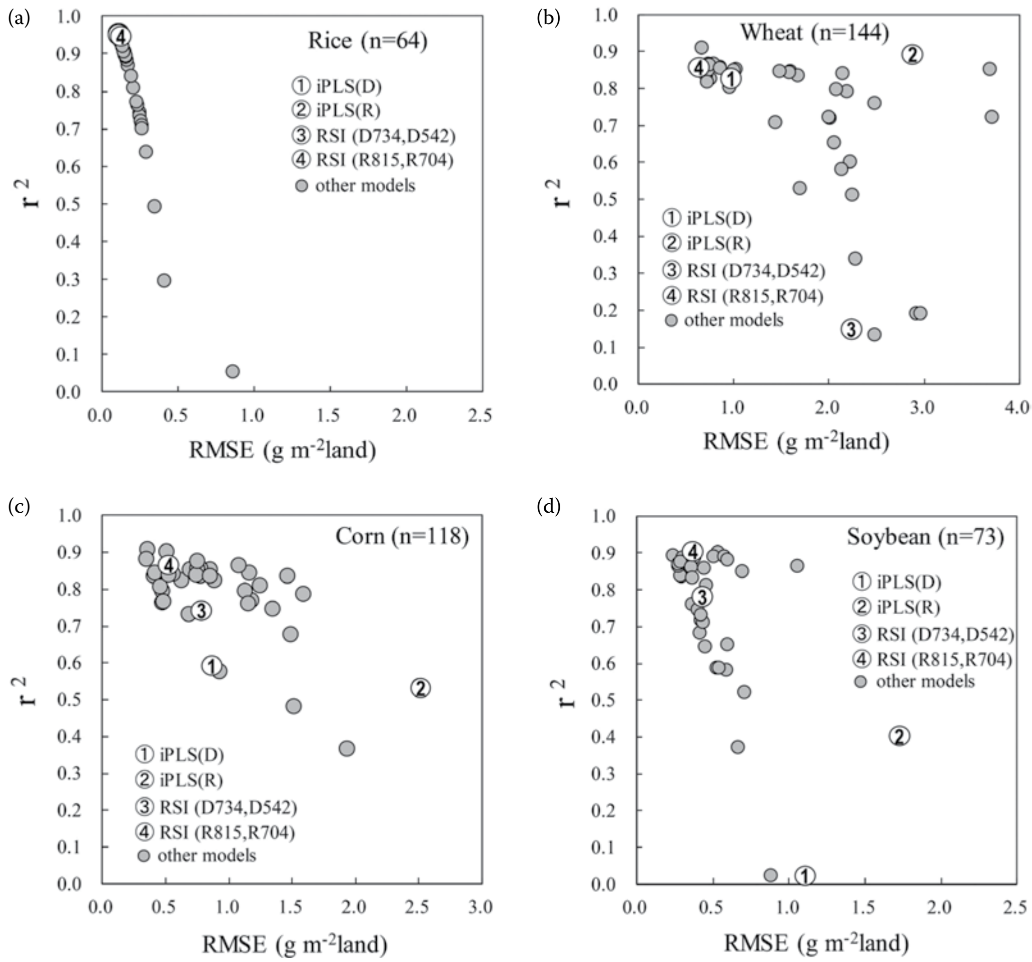

FIGURE 2.15 Applicability of 40 spectral models determined for rice a dataset to the other datasets (rice, wheat, corn and soybean) as indicated by coefficient of determination (r^2) and root mean-square error (RMSE). The best four spectral models obtained for the rice dataset are indicated by symbols with number. Definition of the previous models can be found in the references Vogelmann et al. (1993), Gitelson and Merzlyak (1997), Gitelson et al. (1997), Zarco-Tejada et al. (2001), Peñuelas et al. (1995), Rouse et al. (1974), Huete (1988), Gitelson et al. (2005), Gitelson et al. (2003), Sims and Gamon (2002), Daughtry et al. (2000), Dash and Curran (2004), Huete et al. (2002), Jongschaap and Booij (2004), Lee et al. (2008), Inoue et al. (2012b), and Wang et al. (2003). (After Inoue, Y. et al., 2016. *Plant, Cell and Environment*, 39, 2609–2623.)

Bongiovanni and Lowenberg-Deboer, 2004). Rice (*Oryza sativa* L.) is an important crop for global food security, and the assessment of canopy nitrogen content (CNC) in rice is critical for growth diagnosis and precision management to generate higher yield and better grain quality while also minimizing adverse environmental impacts. Generally, agricultural applications such as precision farming are relatively more demanding than the other applications in terms of accuracy, timeliness, and spatial resolution (Moran et al., 1997; Inoue, 2003; Baret et al., 2007; Asner et al., 2011).

A number of remote sensing approaches have been proposed for the assessment of CNC (e.g., Takahashi et al., 2000; Lee et al., 2008; Sripada et al., 2008; Zhu et al., 2008), but their accuracy and robustness may be inadequate for practical use at regional scales. Previous spectral indices may not be optimized using the merits of data richness and continuity of hyperspectra (Inoue et al., 2008a). Moreover, chemometric approaches such as a partial least-squares regression (PLSR; e.g., Takahashi et al., 2000) may not always be useful.

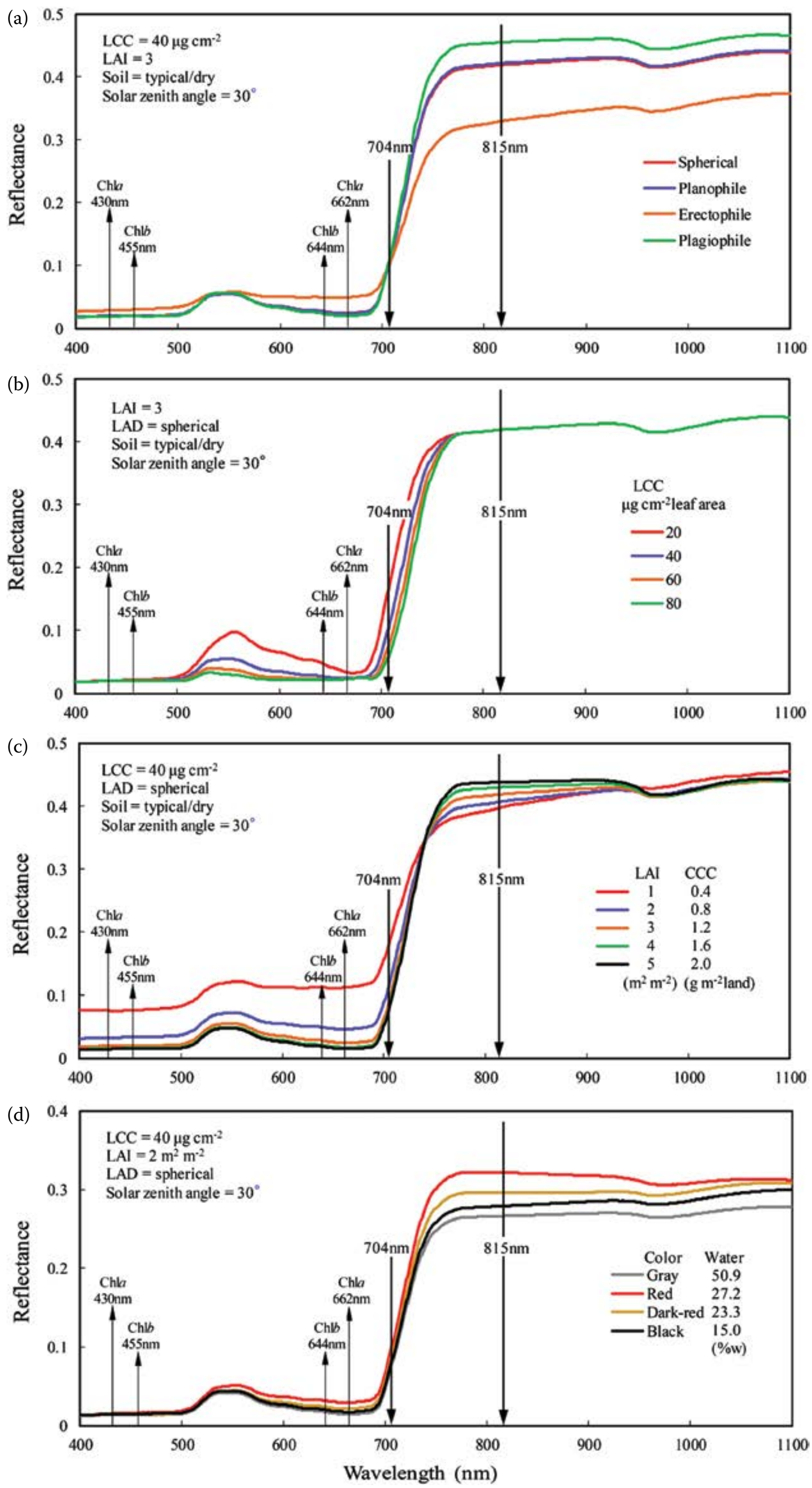

FIGURE 2.16 Reflectance spectra simulated by a physically based canopy reflectance mode PROSAIL under a wide range of plant and soil conditions, namely, different leaf angle distribution (a), leaf chlorophyll concentration (LCC) (b), leaf area index (LAI) (c), and soil color and water content (d). (After Inoue, Y. et al., 2016. *Plant, Cell and Environment*, 39, 2609–2623.)

The study by Inoue et al. (2012b) on the optimal algorithms for remote sensing of CNC in rice (*Oryza sativa* L.) based on diverse *in situ* plant measurements and ground-based and airborne hyperspectral data represents an interesting case study for hyperspectral remote sensing of CNC. Their comprehensive analysis based on the generalized spectral index approach (NDSIs and RSIs) and multivariable regression approach (PLSR and iPLSR) revealed a predictive ability for spectral methods and found promising new spectral indices (Figure 2.17). Among the 20 indices that use the reflectance values at two wavelengths, three indices explored in this study, that is, NDSI(R_{825}, R_{735}), RSI(R_{825}, R_{735}), and SAVI(R_{825}, R_{735}), showed significantly high predictive ability (small RMSE). Although most indices from the literature used the red edge bands, only one index, the CI red edge (Gitelson et al., 2005), showed comparable predictive ability to the three indices. Out of the 12 indices using three to five wavebands, mSR705, VOG-2, MTCI, and VOG-3 showed relatively high predictive ability. Most of these indices also used the red edge wavebands in part, but they were not superior to the three indices using R_{825} and R_{735}. Nevertheless, when derivatives were available, a

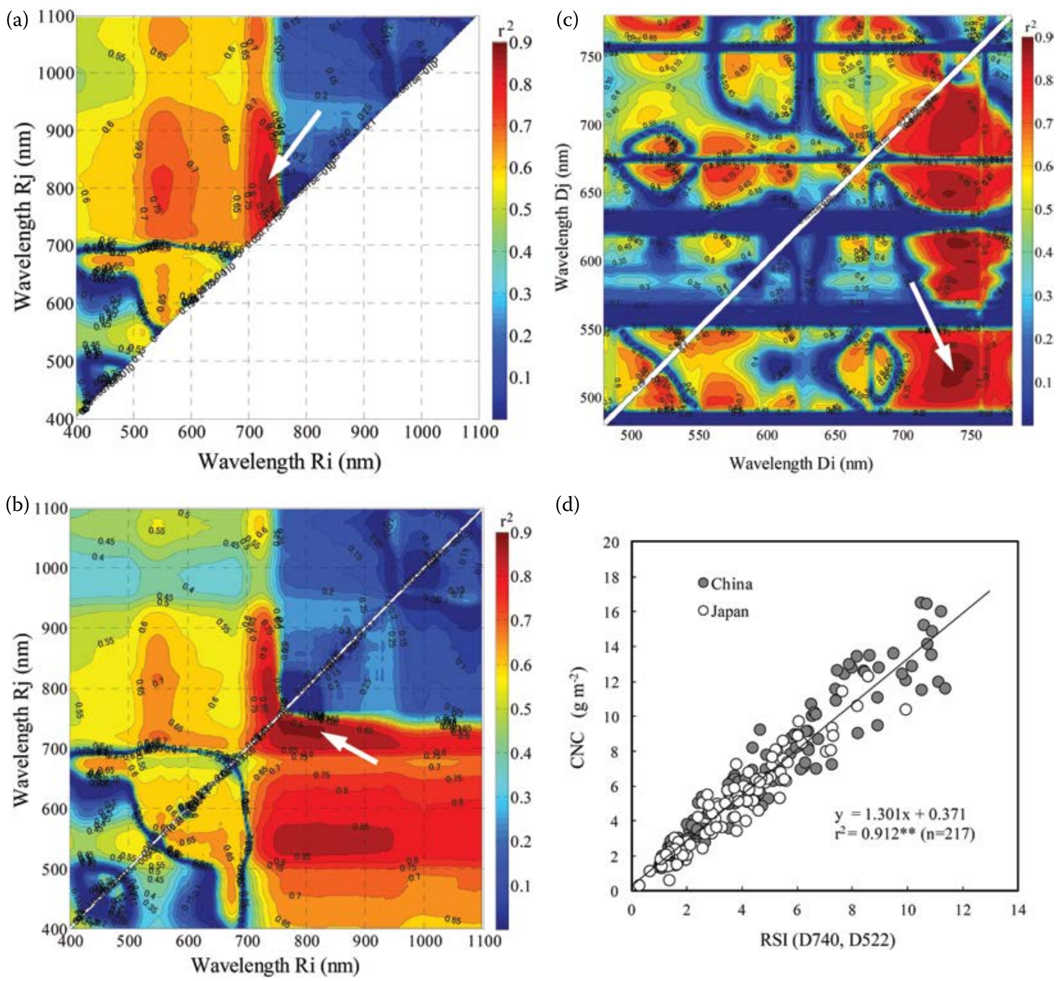

FIGURE 2.17 NDSI and RSI maps of predictive ability for canopy nitrogen content (CNC). (a) NDSI using reflectance values; (b) RSI using reflectance values, (c) RSI using derivative values, and d) relationship between RSI(D_{740}, D_{522}) and CNC for the datasets in China and Japan. ** Indicates the statistical significance at 0.001. The white arrows indicate the most significant spots. (After Inoue, Y. et al. 2012b. *Remote Sensing of Environment*, 126, 210–221.)

simple ratio index RSI(D_{740}, D_{522}) using the first derivative (D) values at 740 and 522 nm, was found to be most accurate and robust for the assessment of CNC. It is reasonable that those spectral indices designed for canopy chlorophyll content would have great potential in assessment of CNC because of the close relationship between nitrogen and chlorophyll contents in green leaves (Morita, 1978). However, optimal spectral models for nitrogen and chlorophyll contents would be different because their relative relationship changes depending on growth stage and nutritive conditions and because the reflectance spectra change differently in response to the ecophysiological changes in nitrogen and chlorophyll contents.

The multivariable models showed a high predictive ability; however, iPLSR using selected wavebands (24% of all wavebands) was superior to PLSR using all wavebands. The predictive ability of iPLSR was comparable to the simple index RSI(R_{825}, R_{735}). The independent validation using the airborne dataset also demonstrated the excellent performance of the simple index RSI(D_{740}, D_{522}) in diagnostic mapping of CNC at a regional scale.

Since nitrogen is a key element for protein and chlorophyll in green plants and thus important for animal nutrition, precise monitoring of CNC would be useful in various applications such as crop and grass management and habitat assessment. These results suggest the strong potential of the new SIs for the assessment of nitrogen content in various plant canopies. The model is now applied to the diagnostics for fertilizer management in rice at regional and farm scales using satellite or drone-based multispectral images (Inoue, 2017; Inoue and Yokoyama, 2017; see Section 2.7.2).

2.5.3 Protein Content of Rice Grain for Production of High-Quality Rice

The protein content of grain (GCP) in rice and wheat is an important quality parameter that affects the price of products (Sakaiya and Inoue, 2013). Higher GCP is valuable in wheat, but lower GCP is preferable in rice because protein content is inversely related to the taste of cooked rice. For example, in rice, GCP is a critical indicator in quality control for regional branding and marketing strategies in several countries such as Japan, Korea, and Taiwan.

However, GCP varies considerably between regions and individual paddies because it is affected by ecophysiological processes such as translocation of nitrogen as well as environmental and management practices during the growing season. Therefore, acquisition of spatial information on GPC in each rice paddy before harvesting is quite useful for regional branding strategies. Such information is used for optimizing the harvest scheduling for better quality, and as a basis for optimizing fertilizer management in the following season. This may be a unique application of remote sensing in agriculture, but would provide some insights for extending the application opportunities of remotely sensed data.

Since the GCP is not incorporated explicitly in any biophysical or physiological models, the generalized spectral index approach using hyperspectral data would be the most feasible to create the optimal predictive algorithms (Inoue et al., 2008a). Figure 2.18 shows the NDSI map of predictive ability for GCP created from hyperspectral data by an airborne sensor (CASI) during the ripening period. The combinations of wavebands in the 530–600 and 710–1050 nm regions have high predictive ability and two hot spots are found on the NDSI map. The best capability was found around the peak of NDSI(R_{970}, R_{570}) with a spectral width of ±20 nm. The significant contribution of R_{970} nm was due to the apparent relation of water content with GCP since water has a specific absorption peak at 970 nm (see Section 2.2). The wavelength region for Landsat NDVI with Landsat bands is between the two peaks and showed relatively low predictive power. The problem of multicollinearity (over-fitting) in MLR is clearly shown in Figure 2.19, where RMSE is smallest in calibration but largest in validation results. It is interesting that the best NDSI(R_{970}, R_{570}) has comparable or better predictive ability than PLSR using the whole spectra or MLR using four selected bands. Another important result is that the iPLSR with band selection had higher ability than PLSR; meaning that the use of whole hyperspectra

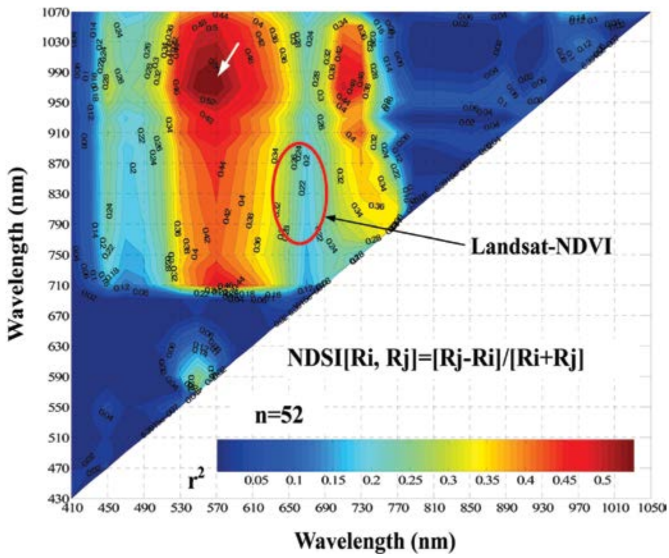

FIGURE 2.18 A contour map of coefficient of determination (r^2) between protein content of rice grain (GPC) and NDSIs. The ellipse indicates the spectral region equivalent to the NDVI using Landsat bands (660 ± 30 and 830 ± 70 nm). (After Inoue, Y. et al., 2008a. *Journal of the Remote Sensing Society of Japan*, 28, 1–14.)

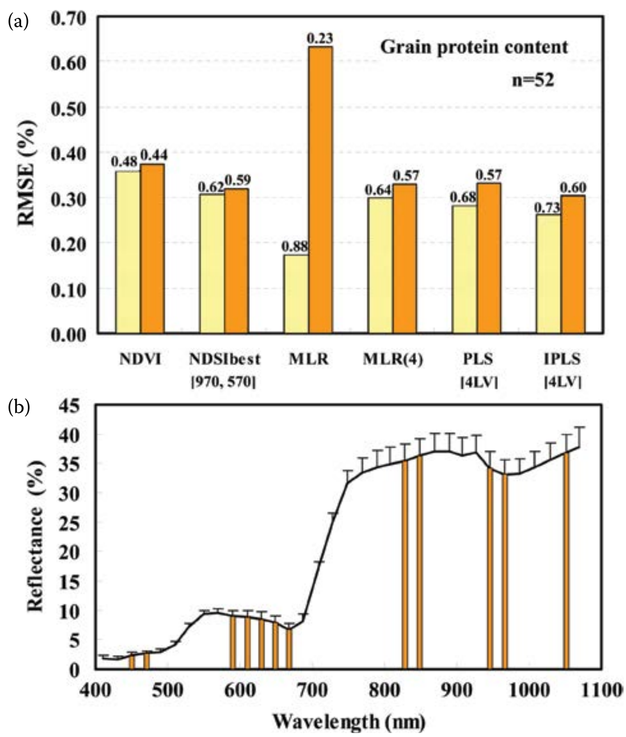

FIGURE 2.19 Comparison of predictive ability in several methods for hyperspectral assessment of grain protein content in rice. (a) RMSEs in calibration (left bars) and in validation (right bars) are shown with coefficient of determination (R^2). The NDSI(R_{970}, R_{570}) was the best NDSI extracted from the NDSI map in Figure 2.18. The values with "LV" in the PLS methods indicate the number of latent variables. (b) Selected 12 wavelengths for the iPLSR model in the average spectra with standard deviation bars for sampled paddy fields. (After Inoue, Y. et al., 2008a. *Journal of the Remote Sensing Society of Japan*, 28, 1–14.)

does not always provide the best result or may be even worse for prediction, presumably because of some erroneous or disturbing spectral bands. The iPLSR method may be useful, but simple indices selected by systematic methods such as NDSI maps would also be useful when only a small number of wavebands are available. These SI models are now applied successfully to the regional-scale management of high-quality rice production using satellite images (Inoue, 2017).

2.6 SPECTRAL ASSESSMENT OF BIOCHEMICAL AND BIOPHYSICAL PROPERTIES IN GRASSES AND TREES

Biochemical and biophysical traits provide understanding about the functional strategies of plants (Colgan et al., 2015). Due to their role in the photosynthetic process, they have close interactions and co-vary across plant functional types (Wright et al., 2004). Many of these traits have been recognized as fundamental functional traits for biodiversity monitoring (Pereira et al., 2013; Skidmore et al., 2015). Biodiversity research from species diversity is moving toward functional diversity (Tilman, 2001), therefore, accurate assessment of these traits is of prime importance.

Detailed hyperspectral studies have revealed that in natural ecosystems such as forests and grasslands, the spectral signature of plants, neglecting the peripheral factors, are mainly altered by change in their biochemical and biophysical properties (Ferwerda et al., 2005; Mutanga and Skidmore, 2007; Cho et al., 2008; Darvishzadeh et al., 2009; Wang et al., 2015b; Ali et al., 2016b; Neinavaz et al., 2016b). These changes are mainly caused by plant growth, health status and stress caused by infestation, pest, and diseases (Hinzman et al., 1986; Zarco-Tejada et al., 2002; Abdullah et al., 2018). Confounding effects such as canopy architecture and background soil are among the most prominent factors affecting the reflectance of vegetation canopies, and are particularly pronounced in sparse canopies. For instance, the effect of soil brightness on the canopy reflectance in a sparse canopy is presented in Figure 2.20. As can be observed from this figure, the variation of background soil in a vegetative canopy has led to differences in canopy reflectance and has caused distinct reflectance offsets in the first derivatives.

A large number of studies have investigated the relationships among the leaf traits. The strengths of these relationships vary across ecosystems and functional types and depend on whether they are expressed on mass or area basis (Wright et al., 2004; Asner and Martin, 2009; Homolová et al., 2013).

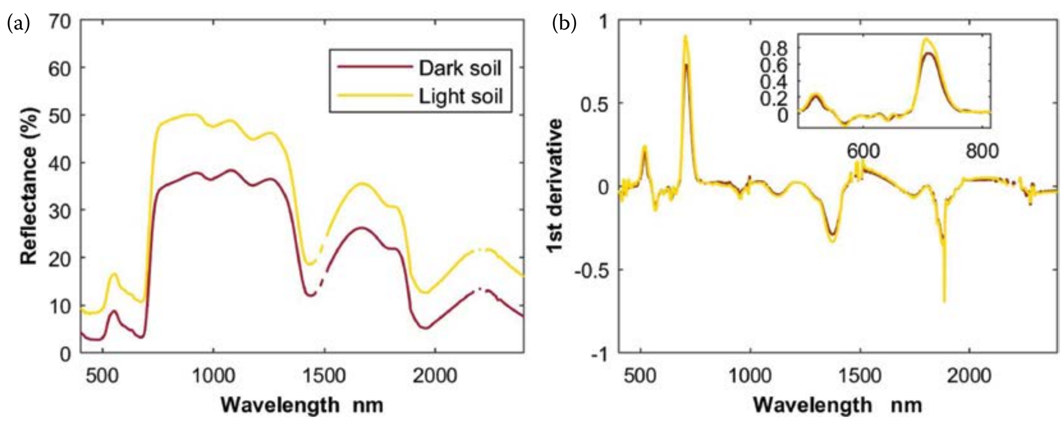

FIGURE 2.20 (a) Spectral reflectance for *Asplenium nidus* canopy with an LAI of 1.5 in dark and light soils; (b) first derivative of the reflectance. (From Darvishzadeh, R. et al. 2008a. *International Journal of Applied Earth Observation and Geoinformation*, 10, 358–373.)

However, it has been observed that area-based leaf traits are generally retrieved with higher accuracy from optical remote sensing data (Wang et al., 2015a), which is due to their role in photosynthesis and processes such as light interception and transpiration that expressed as flux per unit leaf surface area (Hikosaka, 2004; Lloyd et al., 2013).

Among the leaf traits, chlorophyll is the most prominent leaf biochemical that an important role in verifying vegetation physiological status and health, and has been recognized as an indicator for photosynthetic capacity, productivity and detection of vegetation stress (e.g., Carter, 1994; Boegh et al., 2002; Abdullah et al., 2018) (see Section 2.6.1 and Figure 2.21). A wide range of studies have observed moderately strong relationships between chlorophyll and foliar nitrogen, for example (Field and Mooney, 1986; Mutanga and Skidmore, 2007; Kokaly et al., 2009). Therefore, leaf chlorophyll has been suggested as an operational proxy for nitrogen content and vice versa (Muñoz-Huerta et al., 2013). Foliar nitrogen is also related to leaf mass per area (LMA) across different ecosystems, for example (Rosati et al., 2000; Wright et al., 2004; Wang et al., 2015a). LMA is the inverse of specific leaf area (SLA) and provides information on the spatial variation of photosynthetic capacity in addition to leaf nitrogen (Pierce et al., 1994). Since LMA is highly related to the amount of leaf water content (Ali et al., 2016c) (see Section 2.6.2), it can be concluded that leaf water content is linked to other leaf traits such as nitrogen and chlorophyll. As such its relation with foliar nitrogen is demonstrated by Wang et al. (2015a). However, this relationship is vigorous due to the strong temporal dynamic of leaf water content in leaves (Ustin, 2013).

Among canopy biophysical parameters, leaf area index (LAI), in addition to leaf angle distribution and canopy gaps, plays a key role in the magnitude of canopy reflectance (Darvishzadeh et al., 2008a) (see Section 2.6.3). The interrelationship among canopy biophysical traits in forest stands has been documented in several studies. For instance, strong relationships between LAI and biomass, stem density, diameter at breast height (DBH), above-ground net primary productivity (NPP) and canopy cover fraction have been observed (e.g., Hall et al., 1995; Lefsky et al., 1999; Naesset et al., 2005; Schlerf and Atzberger, 2006; Huesca et al., 2016). Moreover, LAI has shown significant correlations with a number of leaf traits such as SLA and leaf nitrogen (Pierce et al., 1994), and leaf dry matter (Ali et al., 2016a). Although the strengths of these relationships are ecosystem and species dependent,

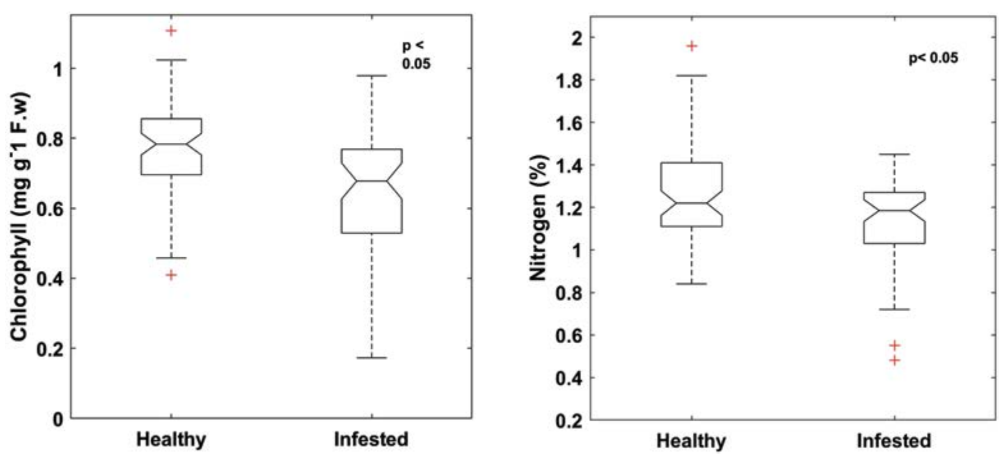

FIGURE 2.21 Distribution of measured chlorophyll and nitrogen concentration for healthy needles and needles infested by bark beetle at the green attack stage. There is a significant difference ($p < 0.05$) in chlorophyll and foliar nitrogen concentration between healthy and infested samples. Infestation decreased mean chlorophyll and nitrogen. (From Abdullah, H. et al., 2018. *International Journal of Applied Earth Observation and Geoinformation*, 64, 199–209.)

these co-variation relations have a key role in evaluation and understanding of their spectral responses (Ollinger et al., 2008).

Studies performed in grasslands and forest (see Section 2.6.2) on leaf traits such as specific leaf area (SLA), leaf mass per area (LMA), and water content have shown sensitivity to wavelengths in the shortwave infrared (SWIR) region of the electromagnetic spectrum (1200–2500 nm) (Ali et al., 2017a,b; Mirzaie et al., 2014; Romero et al., 2012). While the spectral bands sensitive to foliar chlorophyll and carotenoids, exist in the visible and red edge region (400–750 nm) (Curran, 1989; Dawson et al., 1999), leaf nitrogen has been related to different spectral regions (Curran, 1989; Fourty et al., 1996; Kokaly et al., 2009; Ollinger et al., 2008; Knyazikhin et al., 2013; Wang et al., 2017). This may be explained by the interrelation and interactions of leaf nitrogen with other leaf and structural traits. Thus Wang et al. (2017) demonstrated that in spruce stands the sensitive bands for estimating foliar nitrogen in the visible region are mainly related to chlorophyll absorption, while in the near-infrared (NIR) and SWIR regions, the bands sensitive to foliar nitrogen are explained by the existence of protein and dry matter content as well as biological associations between nitrogen and structural traits.

Knowledge of biophysical and biochemical traits and their variations in natural ecosystems is critical for many management practices such as biodiversity monitoring, climate modeling, and carbon cycle assessment. The following subsections present a few scenarios in which, utilizing hyperspectral measurements, accurate estimations of these parameters in the forest and grasslands have been made.

2.6.1 Leaf Biochemical Properties for Detection of Insect Outbreaks in Forest

European spruce bark beetle (*Ips typographus* (L.)) is the most aggressive forest insect pest in the European forests, and they can destroy many more forested areas than all other natural disturbances. The extent of bark beetle damage has been huge, and trees have been killed over tens of millions of hectares, causing a great economic loss in timber production. In addition, a large amount of public money has been expended in clearing the fallen trees. Further, insect outbreaks have resulted in significant ecological changes in terms of the forests' structure and composition, wildlife habitats, and degradation of large areas within these forests. To meet the information requirements to minimize economic losses and to preclude further mass outbreaks, early detection of insect outbreak is vital (in a period in which trees are yet to show visual signs of infestation stress). This information plays a vital role in forest management and is critical when developing sustainable forest management policies and conservation strategies. Visual inspections during field surveys and pheromone traps traditionally have been used for detection of bark beetle infestation in Norway spruce forests. However, these methods are subjective, time-consuming, and ineffective for low-level infestation (i.e., not an outbreak). Consequently, acquisition of remote sensing data is a proper alternative for developing new techniques for monitoring and detecting this forest disturbance.

Physiological studies have indicated that biochemical variables such as leaf water, chlorophyll, and nitrogen contents are the main properties of the plants that are sensitive to both environmental conditions and insect infestation and have a direct impact on leaf and canopy optical properties (Gitelson et al., 2003; Munoz-Huerta et al., 2013). Accordingly, biochemical variables play a key role in plant growth and photosynthesis and are considered as indicators of plant health and stress. In recent decades, many studies have shown the role of remote sensing, in particular hyperspectral imagery, in measuring vegetation biochemical variables such as chlorophyll and nitrogen content in different ecosystems (Asner and Martin, 2009; Asner et al., 1998; Darvishzadeh et al., 2008b; Wang et al., 2015a). Therefore, hyperspectral measurements integrated with biochemical properties have been considered to study the forest insect outbreaks. Abdullah et al. (2018), have used foliar reflectance and biochemical propitiates (chlorophyll and nitrogen content) to detect early stage of bark beetle infestation in the Norway spruce forests in Central Europe. In their study, partial

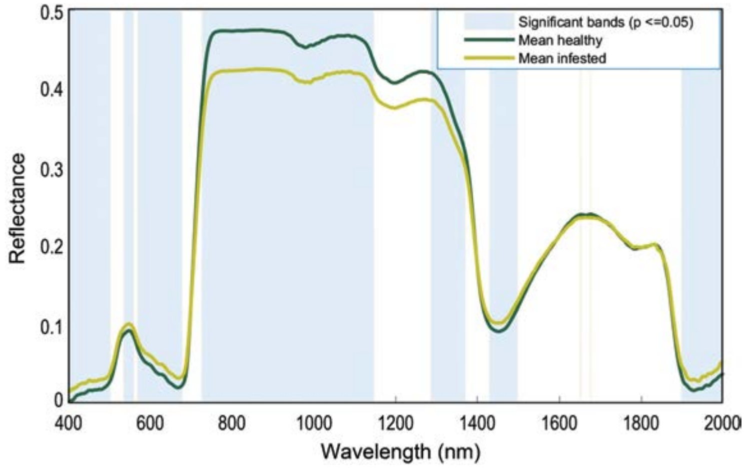

FIGURE 2.22 Mean reflectance spectra of healthy and infested leaves of European spruce at the green attack stage (see Fig. 2.22). Tinted areas depict the location of wavebands displaying is a significant difference between healthy and infested spectra. (From Abdullah, H. et al., 2018. *International Journal of Applied Earth Observation and Geoinformation*, 64, 199–209.)

least-square regression (PLSR) was utilized to assess the impact of infestation stress on the retrieval accuracy of foliar biochemical properties. They found that bark beetle infestation at the early, so-called green attack, stage (when the leaves are still green and not visibly stressed) affects the leaf spectral response as well as leaf biochemical properties and their retrievals from hyperspectral measurements (Figure 2.22). They concluded that the assessment of retrieval accuracy of these two biochemical components could be used as an indicator for the efficient landscape-wide detection of the early stage of bark beetle infestation.

Not only chlorophyll and nitrogen content but also leaf water content can be used as a proxy to detect bark beetle infestation. Cheng et al. (2010) used leaf water content to detect pre-visible mountain pine beetle damage in lodgepole pine needles using hyperspectral measurements. They concluded that the measurable water deficit of infested tree samples was detectable from a narrow spectral region (1318–1322 nm) and could be used to distinguish between healthy and infested trees by mountain pine beetle.

Although detecting the early phase of insect outbreak in the Norway spruce forests is challenging using remote sensing data, due to the lack of apparent visual symptoms on the affected trees, quantifying biochemical variables from hyperspectral measurements is promising and presents a powerful tool to determine the damage caused by bark beetle green attack at the leaf level. In other words, the information obtained about biochemical variables using hyperspectral measurements is sufficient to detect insect outbreaks in the forest at an early phase.

2.6.2 Assessment of Leaf Functional Traits in Forest (SLA and LDMC)

Quantifying functional traits in natural communities is pivotal to understanding the spatial and temporal distribution of biodiversity, ecosystem services, and plant community productivity (Cadotte et al., 2011; Lavorel et al., 2011). Since human survival relies on economic benefits and services provided by ecosystems, it is evident that ecosystem functions are a top conservation priority. Scientists believe that better conservation and restoration decisions can be made by measuring and understanding functional traits (Cadotte et al., 2011). Remotely sensed data can play a critical role in acquiring such functional traits data over broad spatial scales nondestructively and repeatedly. Ali et al. (2016a,b, 2017a,b) elucidated the potential of remotely sensed data to quantify two fundamental leaf functional traits (i.e., leaf dry matter content [LDMC] and specific leaf area [SLA]) in a mixed forest at leaf, canopy, and landscape scales by using statistically and physically based predictive models.

The leaf-level study by Ali et al. (2016b) through inversion of the most commonly used leaf radiative transfer model PROSPECT (Jacquemoud and Baret, 1990) revealed accurate estimation of the two leaf traits in a wide range of samples collected from broadleaf and conifer forest stands. Validation of the two leaf trait estimations showed the high coefficient of determination (R^2) between the predicted and ground measured values ($R^2 = 0.83$ for LDMC and $R^2 = 0.89$ for SLA). The results showed that the PROSPECT_4 leaf model accurately simulates spectral information of samples from mixed mountain forest and can be used to retrieve the biochemical content of leaves/needles directly and indirectly through inversion over a range of vegetation types. It highlighted the fact that LDMC and SLA are quantitatively represented by leaf spectra. This leaf-level result sheds light on extending or upscaling the application of remotely sensed data in order to accurately estimate the two functional traits at canopy and landscape scales.

There are no well-developed methods for fast and accurate retrieval of LDMC and SLA at canopy or larger scales. Hence, both the statistical and physical approaches were investigated in order to map the two leaf traits in a mixed mountain forest, using the hyperspectral HySpex airborne images and the multispectral Landsat-8 Operational Land Imager (OLI) data (Ali et al., 2017b). The spectral features that have high correlations with LDMC and SLA were identified by applying continuous wavelet analysis to INFORM-simulated canopy spectra (Atzberger, 2000). The application of continuous wavelet analysis resulted in six sensitive wavelet features for LDMC and four for SLA being in the top 1% strongly correlated wavelet features. The results indicated the capability of the wavelet transformation to identify the most sensitive spectral features from a large hyperspectral dataset and the robustness of wavelet transformation in creating a higher correlation of wavelet features to vegetation variables compared to use of nontransformed original spectra (Figure 2.23). This may be attributed to the effectiveness of wavelet analysis in decomposing the trait's absorption features into various scales of narrow- and broad-band absorption features and identifying those that correlate best with the variation in the traits' concentration.

The suitability of indices for SLA retrieval at leaf and canopy levels for heterogeneous mountain forest has been evaluated by Ali et al. (2017b). The correlation tended to be lower at the canopy level, and many of band combinations that showed a high correlation to SLA at leaf level became

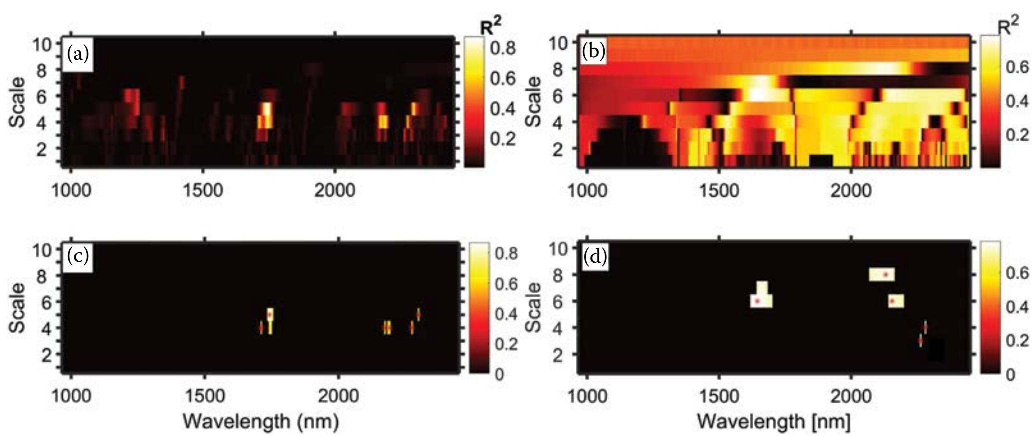

FIGURE 2.23 Correlation scalograms for the identification of wavelet features that significantly correlate with (a) leaf dry matter content (LDMC) and (b) specific leaf area (SLA). Scalograms are derived from continuous wavelet analysis of simulated spectra. Brightness represents the coefficient of determination (R^2) relating wavelet power to LDMC and SLA. Colored regions in scalograms (c) and (d) depict the wavelet features with the top 1% greatest R^2 values for LDMC and SLA. (From Ali, A.M. et al., 2016c. *ISPRS Journal of Photogrammetry and Remote Sensing*, 122, 68–80.)

insensitive at canopy scale. Although only narrow-band indices were examined, our findings suggest that bands with a wider wavelength range (broad bands) can be utilized. This implies that remote sensing data from coarse spectral resolution sensors may suffice for SLA estimation.

In the study by Ali et al. (2017b), SLA was retrieved from the recently launched Landsat-8 imagery by empirical methods (individual bands and vegetation indices) and the inversion of the INFORM radiative transfer model through wavelet transformation and lookup table approaches in order to explore the potential of medium-resolution multispectral satellite images to predict SLA for a mixed mountain forest (Ali et al., 2017b). It was evaluated whether the methods earlier studied at leaf and canopy scale using hyperspectral field and airborne data can be utilized at a larger scale using medium-resolution satellite data. Both the statistical and INFORM inversion predicted SLA with satisfactory accuracy.

The findings and methods of these studies have the potential to produce useful information from hyperspectral and multispectral remote sensing data about leaf functional traits at local, regional, and global scales. The results further confirmed the applicability of remote sensing to elucidate variation in general ecological leaf functional traits across relevant spatial and temporal scales. This will facilitate regular monitoring of biodiversity, particularly with respect to natural or anthropogenic changes in ecosystem functioning.

2.6.3 Analysis of Biophysical and Biochemical Traits in Grasslands

In natural heterogeneous canopies such as grasslands, where the species diversity is high, the reflectance is often a mixture of different species; hence, remote sensing applications are challenging. A detailed investigation is required to assess the aptitude of remote sensing models when it comes to the combination of different plant species in varying proportions. The utility of hyperspectral remote sensing in predicting leaf and canopy characteristics such as LAI and canopy and leaf chlorophyll content in a heterogeneous Mediterranean grassland by different modeling approaches (statistical and radiative transfer models) at laboratory, field, and airborne levels was studied by Darvishzadeh et al. (2008a,b).

A number of key observations about the effects of canopy heterogeneity on retrieval of traits were made for analysis using statistical models. It was observed that unlike most common vegetation indices where the near-infrared (NIR) region is the keystone, wavebands from the short-wave infrared (SWIR) region contained most relevant information about canopy LAI, and the "hot spots" (regions where the sensitive band combinations exist) mostly occurred in this spectral region at laboratory, field, and airborne levels. This emphasized that the vegetation indices that do not include the SWIR spectral region may be less satisfactory for LAI estimation (Darvishzadeh et al., 2008b). Moreover, the results suggested that not only the choice of vegetation index but also prior knowledge of plant structural components and the background soil are important when using vegetation indices for LAI estimation (see Figure 2.20). Accordingly, landscape stratification is required when using hyperspectral imagery for large-scale mapping of vegetation biophysical variables.

Radiative transfer models have rarely been used for studying heterogeneous grassland canopies. The widely used PROSAIL (Verhoef, 1984, 1985; Jacquemoud and Baret, 1990; Kuusk, 1991) model by means of a lookup table (LUT) was utilized by Darvishzadeh et al. (2008b) with a number of stratifications to overcome the ill-posed nature of the model inversion and improve the retrievals of LAI, and leaf and canopy chlorophyll content. Their results showed that canopy chlorophyll content was predicted with the highest accuracy ($R^2 = 0.70$, normalized RMSE = 0.18), while LAI was estimated with moderate accuracy ($R^2 = 0.59$, normalized RMSE = 0.18). Heterogeneity had a pronounced effect on inversion algorithm and the retrieval of these parameters. Hence, the stratification of data based on the number of species increased the estimation accuracies of these parameters. The accuracy systematically fell each time sample plots with more (up to four) species were included in the inversion process. This demonstrated the limitations of the PROSAIL radiative transfer model when the spectral reflectance stems from a rather heterogeneous vegetation canopy condition. When a limited number of wavelengths corresponding to various vegetation parameters and bands showing low average absolute errors were used for model inversion, the relationships between estimated and measured grass variables were comparable to those obtained from all wavebands. This indicated that a carefully chosen spectral subset contains sufficient information for a successful model inversion and can improve the ill-posed nature of the model inversion.

Utilizing canopy reflectance, leaf chlorophyll content could not be estimated with an acceptable accuracy exploiting either of the modelling approaches. Leaf biochemical variables suffer from poor signal propagation from leaf to canopy scale (Yoder and Pettigrew-Crosby, 1995; Jacquemoud et al., 1996; Asner et al., 1998), with only few exceptions (Jacquemoud et al., 2009; Xiao et al., 2014). Therefore, their retrieval from canopy reflectance is challenging (Darvishzadeh et al., 2008b). At the canopy level, biophysical variables such as leaf area index (LAI) and canopy architecture (e.g., leaf angle distribution) presented major contributions to the canopy reflectance, mainly in near-infrared (NIR) and SWIR regions (Darvishzadeh et al., 2009; Ali et al., 2016a). Among these parameters, perhaps LAI has the most prominent role in defining the magnitude of the canopy reflectance, such that increase in LAI values increased the canopy reflectance in NIR and SWIR regions (Figure 2.24a).

The above findings illustrate some possibilities for estimating and mapping LAI and chlorophyll in a rather heterogeneous grassland. However, the application of the methods developed to other heterogeneous biomass and parameters needs to be evaluated using different hyperspectral data sets to explore the scale and sensor effects as well as phenological influences. It was observed that the heterogeneity (species diversity) almost disappeared at the airborne level, as using airborne data the retrieval accuracy of the studied variables increased using either the statistical or the physical model. However, heterogeneity is strongly scale dependent and relative.

2.6.4 Response of LAI to Thermal Hyperspectral Data

The thermal infrared region (TIR 8–14 μm) has traditionally been treated differently from the other parts of the electromagnetic spectrum due to the differences in acquisition, calibration, and processing of the data over this region. Despite the recent advances in the field of thermal remote sensing, this domain has hardly been used for vegetation studies. Consequently, there still is limited and insufficient information regarding the responses of plant traits over TIR domain. The existing

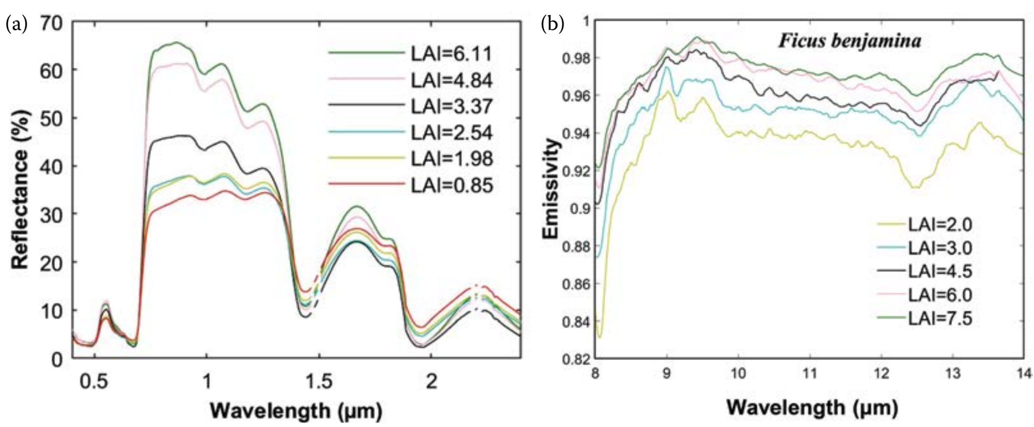

FIGURE 2.24 (a) Canopy spectral reflectance of *Asplenium nidus* in visible, near infrared, and short-wave infrared regions corresponding to LAI values between 0.87 and 6.11. (b) The canopy emissivity spectra in *Ficus benjamina*. Changes in canopy emissivity spectra become smaller when LAI values exceed 4.0 ($m^2\ m^{-2}$). ([a] From Darvishzadeh, R. et al., 2009. *International Journal of Remote Sensing*, 30, 6199–6218; [b] Neinavaz, E. et al., 2016a. *ISPRS Journal of Photogrammetry and Remote Sensing*, 119, 390–401.)

misconceptions over the TIR data are related to relatively inaccessible instruments with high signal-to-noise ratio, and subtle emissivity spectral variations in plants (Ribeiro da Luz and Crowley, 2010). Further, little is known by the ecological and remote sensing communities about plant physiology in association with plant spectral features in the TIR domain (Quattrochi and Luvall, 1999). However, none of these difficulties has reduced the importance of the TIR region, which benefits from a wide atmospheric window with large transparency offering high potential for remote sensing vegetation studies (Clerbaux et al., 2011).

As a result, Neinavaz et al. (2016a,c) explored the potential of hyperspectral TIR canopy measurements to measure and quantify the canopy LAI as the key canopy biophysical property. LAI is strongly associated with numerous ecosystem processes (e.g., water balance and evapotranspiration) and plays a vital role in climate and terrestrial ecosystem models. Additionally, LAI has recently been proposed as one of the essential biodiversity variables (EBVs) that are potentially suitable for satellite monitoring of biodiversity and progress toward the Aichi Biodiversity Targets (Pereira et al., 2013; Skidmore et al., 2015). Moreover, the demand for LAI monitoring over large areas has increased in recent decades due to rising concern over habitat degradation and climate change.

The effect of changing LAI values on canopy reflectance has been investigated and confirmed in a number of studies (Asner et al., 1998; Darvishzadeh et al., 2009) in which it was demonstrated that with increasing LAI the canopy reflectance spectra increases noticeably in the NIR and SWIR regions (Figure 2.24a). The effect of LAI on plant emissivity spectra has only recently been investigated using TIR hyperspectral data by Neinavaz et al. (2016a). In their study the response of vegetation canopies with various LAI values to canopy emissivity spectra was investigated. It was observed that there is a positive relationship between canopy emissivity spectra and LAI and that the emissivity rises with increasing LAI values. This increment was more pronounced beyond the wavelength region of 9 μm (Figure 2.24b). Further, their results revealed that the species with similar LAI values could have distinct canopy emissivity spectra, suggesting that LAI is not the sole parameter that affects the canopy emissivity spectra and that other traits also contribute to these spectra.

The potential of TIR hyperspectral data for estimation of LAI was further explored for four structurally different species in Neinavaz et al. (2016c). The results of their study revealed that LAI and emissivity relations are only statistically significant in some wavebands. Vegetation indices, partial least-square regression (PLSR) and artificial neural networks (ANN) were applied for LAI retrieval in different species; their retrieval accuracies were comparable and the predicted accuracies were highly species dependent and varied among species. The most sensitive wavebands across species were in the 10–12 μm range in combination with the bands in the 8–11 μm range. The predicted LAI from the pooled dataset had lower accuracy than the ones obtained for individual species resulting from variation of biochemical and structural parameters across the species studied.

It is expected that other parameters, particularly those modulated from biochemical and biophysical variables, are likely to have more contribution to canopy emissivity spectra. Recent studies performed in mixed forest stands using TIR remotely sensed data demonstrated that canopy emissivity is a meaningful measure for retrieving vegetation modulated properties, particularly at the canopy level (Neinavaz, 2016a,b,c).

2.7 GENERIC ROLE OF HYPERSPECTRAL DATA FOR ESTIMATION OF ECOPHYSIOLOGICAL FUNCTIONING

2.7.1 Generic Use of Hyperspectral Data for Present, Future, and Past Sensors

In general, calibration and validation of predictive models are essential for higher accuracy and applicability in assessment of biophysical and ecophysiological variables from remotely sensed data. In past decades, a large number of papers have reported predictive algorithms and models using various sensors having different numbers of spectral bands, central wavelength, and bandwidth (Thenkabail et al., 2012). However, their predictive accuracy and applicability are often inconsistent between datasets because of the differences in sensor specifications. A predictive model based on a dataset using a sensor cannot be applied directly to the other sensors. For example, the widely used spectral index NDVI (normalized difference vegetation index) derived from different sensors would not be equivalent to each other because of the differences in position and width of the red and near-infrared wavebands. Some sensors have the red edge band but the others do not, while the band is most useful for assessment of chlorophyll content. Accordingly, calibration and validation procedures are required for individual sensors based on sufficient number of spectral data and reliable *in situ* measurements of biophysical or ecophysiological variables. Such datasets usually have to be acquired by laborious and careful procedures, which would hamper the wide and generalized application of remote sensing. Furthermore, acquisition of such datasets is impossible from the various sensors used in the past even if a large volume of images are available in open archives.

However, precise hyperspectral data of sufficient spectral resolution (1–3 nm) acquired together with the diverse range of target variables would play a generic role in deriving the optimal algorithms and predictive models for various types of sensors of the past, present, and future. Hyperspectral datasets obtained in close range can especially be an accurate basis for various applications because uncertainties due to atmospheric conditions and spatial heterogeneity within a pixel are negligible. Optimal algorithms and predictive models can be derived as default from such datasets for various sensor specifications of satellite-, aircraft-, and drone-based multispectral sensors of the past, present, and future. This hyperspectral approach would be realized through three methods: (1) generalized spectral index method, (2) advanced use of physically based reflectance models, and (3) data-driven machine learning methods. The second and third methods have several constraints as discussed in Section 2.3. Therefore, the first method would be the simplest and most flexible approach.

Figure 2.25 shows a schematic of the generic use of hyperspectral datasets for assessment of ecophysiological functioning of crops and vegetation based on the generalized spectral index method. The generalized spectral index approach, such as NDSI(R_i, R_j), RSI(R_i, R_j) and/or their derivatives using the whole spectral wavebands (see Section 2.3.1), allows one to choose optimal sensors and wavebands from available satellite or drone sensors. In addition, most suitable algorithms and predictive models (formulas and parameters) can be determined for any sensors, even those used in the past. Note that spectral data for this approach have to be precise reflectance data at the target surfaces, so that appropriate radiometric and atmospheric collections are needed.

2.7.2 Strategic Application of Hyperspectral Data to Drone-, Airborne-, and Satellite-Based Multispectral Image Sensors

The number of earth observation satellites with high spatial resolution (under 10 m) has been increasing consistently during the past decade, and is further increasing at a rapid pace. A constellation of hundreds of small satellites is already realized (e.g., Dove satellites by Planet) and many similar programs are planned (Lal et al., 2017). Accordingly, global land surfaces can be observed once a day at high spatial resolution. On the other hand, the availability of small unmanned aerial vehicles (termed drones, UAVs, or UASs) is expanding rapidly worldwide (Zhang and Kovacs, 2012; Stöcker et al., 2017). This platform environment favors the advanced operational applications of remote sensing to assessment of ecophysiological functioning of crops and vegetation. The high spatial resolution and timely data acquisition are the unique advantages of drone-based remote sensing.

Under such a platform environment, the hyperspectral datasets would play a critical role for generating predictive models for any sensors with different specifications, regardless of the availability of satellite hyperspectral sensors (see Section 2.7.1). The generalized spectral index approach would greatly reduce the laborious and careful tasks for creation and validation of predictive models required for advanced use of various sensors with diverse specifications (number of spectral bands, central wavelength, and bandwidth).

Figure 2.26 shows application examples of the generic hyperspectral approach to diagnostic mapping of canopy nitrogen contents by satellite- and drone-based multispectral sensors. The optimal

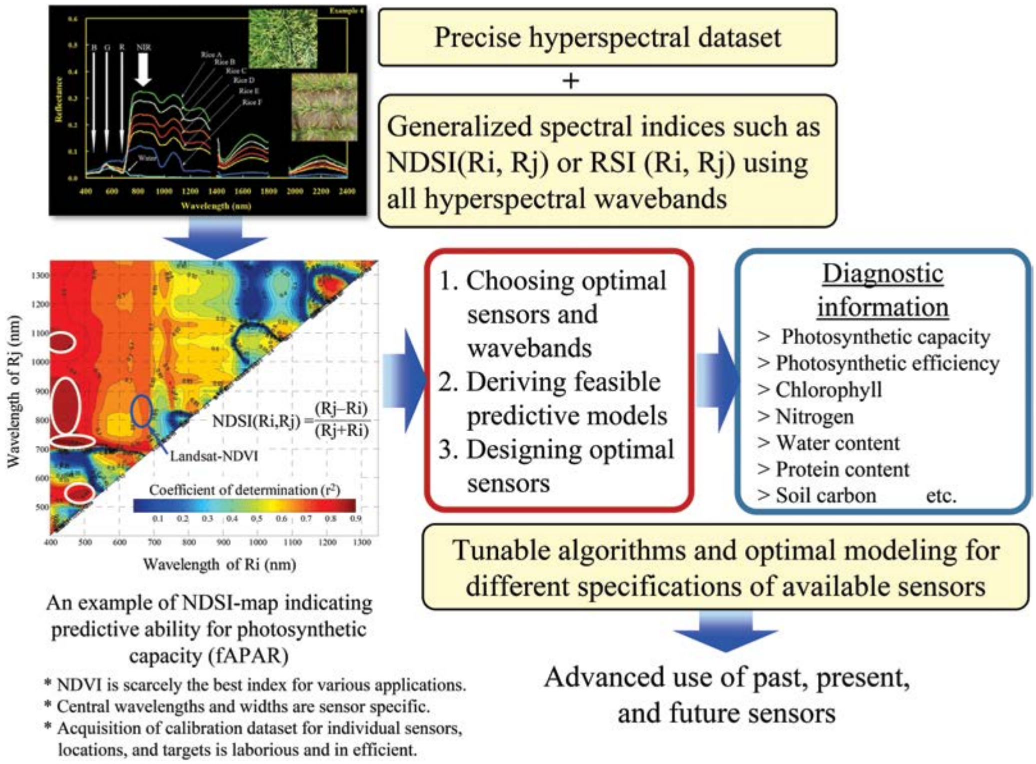

FIGURE 2.25 Schematic representation of the generic role of a hyperspectral dataset for assessment of biophysical and ecophysiological functioning of vegetation. (After Inoue, Y. 2017. *Journal of the Remote Sensing Society of Japan*, 37, 213–223.)

algorithms and predictive models for each sensor were created and validated based on hyperspectral datasets and applied to each sensor for mapping. The scatterplot with each map indicates the results of simple validation with independent *in situ* datasets. These results confirm the robust applicability of the generic approach based on hyperspectral datasets for creation of optimal algorithms and predictive models for individual band specifications. For example, in prediction of chlorophyll content, different optimal (best, second-best, etc.) models can be created in accordance with sensor specifications even with or without the red edge bands. Nevertheless, we should be careful about the quality of multispectral images since all algorithms and predictive models are affected by the accuracy of spectral reflectance. Appropriate radiometric and atmospheric corrections are required for satellite images, and precise radiometric correction and ortho-mosaic processing are needed for drone-based images (Inoue, 2017; Inoue and Yokoyama, 2017).

2.8 CONCLUSIONS AND PERSPECTIVES: DIAGNOSTIC INFORMATION FOR SMART AGRICULTURE AND ENVIRONMENTAL MANAGEMENT

So-called "precision agriculture" (PA) has emerged as one of the advanced technologies in recent decades (Stafford, 2000). GPS and agricultural machines equipped with sensors and variable-rate apparatus are essential for PA. In addition, georeferenced information from remote sensing can play a significant role in PA (Moran et al., 1997; Zhang and Kovacs, 2012) since site-specific management based on the spatial heterogeneity within each field is the central issue for PA. "Smart agriculture" (SA) is a new trend following PA, which is more advanced style of agriculture based on sensing and robotics technologies as well as information and communication technologies (ICT) including big

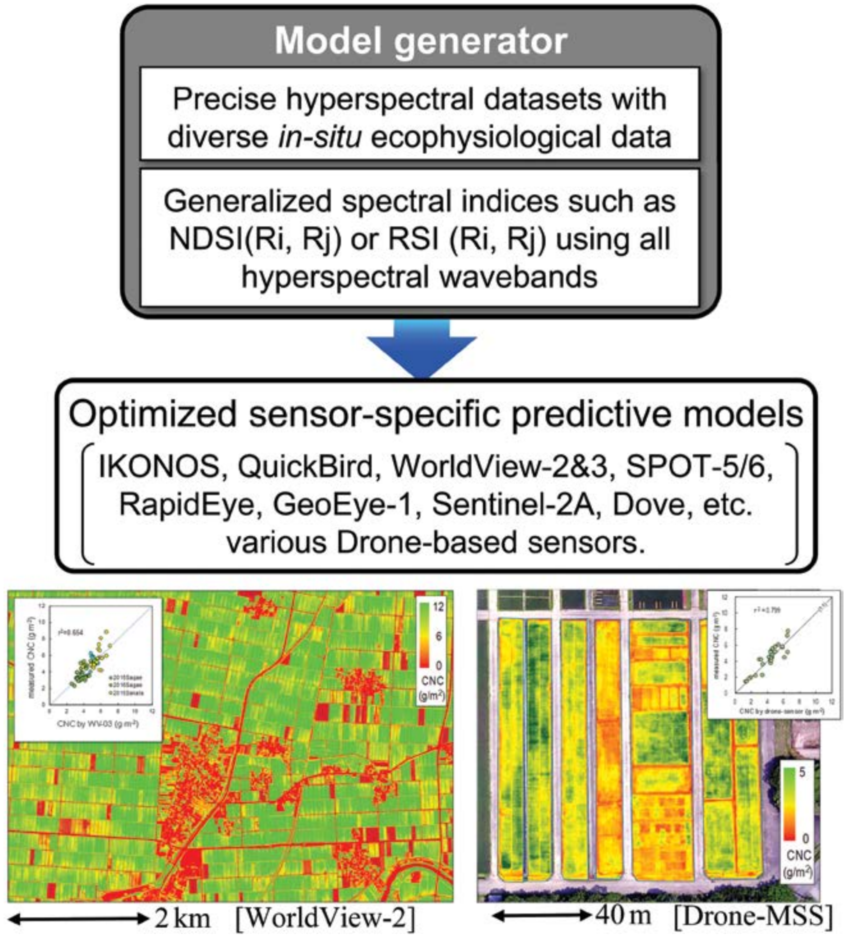

FIGURE 2.26 Application of a generic model generator based on hyperspectral datasets. Examples shows the diagnostic maps of canopy nitrogen content at regional scale by WorldView-2 (left) and drone-based multispectral sensors (right). Optimal predictive models for each sensor were derived from the hyperspectral dataset and calibrated and validated before application to each multispectral sensor. Scatterplots show the independent validation of multispectral estimates using *in situ* data. (After Inoue, Y. 2017. *Journal of the Remote Sensing Society of Japan*, 37, 213–223; Inoue, Y. and Yokoyama, M. 2017. *Journal of the Remote Sensing Society of Japan*, 37, 224–235.)

data and artificial intelligence (Inoue, 2017; Figure 2.27). By making the most of these technologies, SA seeks higher yield and quality with less labor and inputs. Geoinformation from remote sensing will be even more critical in SA as a unique source of spatial data and diagnostic information for optimization of planning and management practices. Accordingly, in SA, ecophysiological information on crop growth such as chlorophyll and nitrogen contents, water stress index, maturity stage, and photosynthetic productivity and/or on soil fertility is needed for optimization of fertilizer application, irrigation management, and harvest scheduling as well as for yield prediction.

On the other hand, remotely sensed information plays an important role in various aspects of environmental policy making (de Leeuw et al., 2010; IPCC, 2014). Especially under conditions of climate change such as increasing atmospheric CO_2 and global warming, mitigation and adaptation strategies are of great concern worldwide. The dynamics of terrestrial vegetation is strongly related to exchange of CO_2, energy, and water between atmosphere and land surface, in which ecophysiological functioning of vegetation plays a critical role. Accordingly, the diagnostic geoinformation on

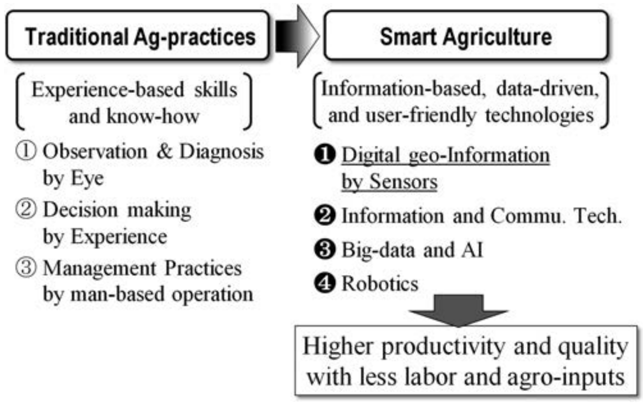

FIGURE 2.27 Innovative technologies needed for transformation from traditional agriculture to smart agriculture, and the role of diagnostic information from remote sensing in smart agriculture. (After Inoue, Y. 2017. *Journal of the Remote Sensing Society of Japan*, 37, 213–223.)

ecophysiological functioning of vegetation at regional or global scales is an essential basis for environmental sciences and policy making. Remotely sensed data are prerequisite for spatiotemporal assessment of carbon cycle in terrestrial ecosystems (Inoue et al., 2010; Thapa et al., 2015; Vadrevu et al., 2018; Figure 2.28). Assessment of biodiversity is also one of the important application areas for hyperspectral remote sensing (e.g., Nagendra et al., 2013; Feilhauer et al., 2017).

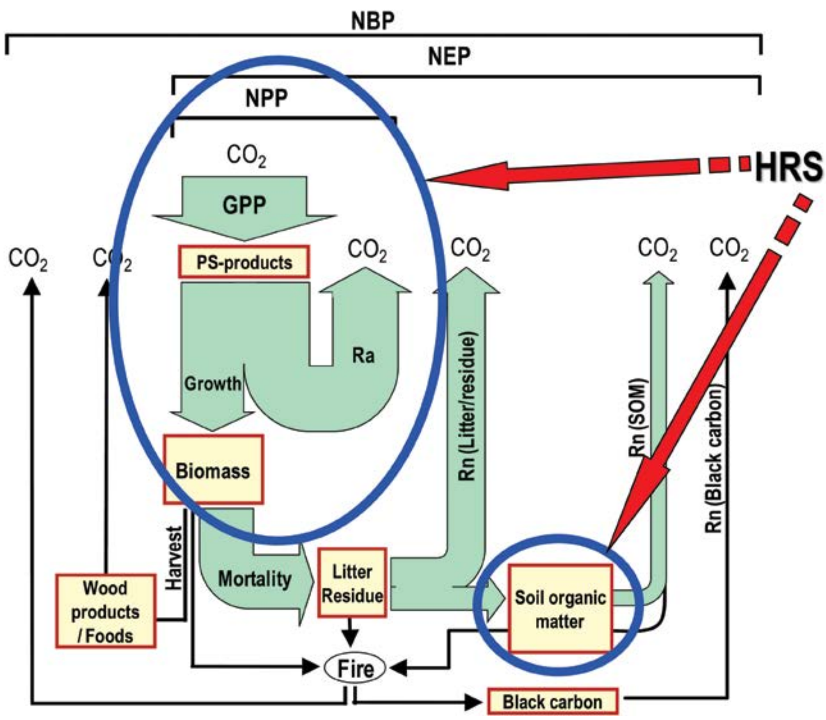

FIGURE 2.28 Hyperspectral assessment of ecophysiological functioning at ecosystem scales for vegetation and carbon cycle sciences as a basis for policy making for land use and environmental conservation. HRS: Hyperspectral remote sensing; GPP, gross primary production; NPP, net primary production; NBP, net biome production; NEP, net ecosystem production. (After Inoue, Y. et al., 2010. *International Journal of Applied Earth Observation and Geoinformation*, 12, 287–297.)

Hyperspectral data enables plant functional information to be acquired that is impossible to acquire with other types of sensors. Further studies on hyperspectral remote sensing of vegetation functioning are needed not only for hyperspectral satellite sensors such as EnMAP and HyspIRI (Staenz and Held, 2012), but also for advanced use of a wide range of multispectral sensors.

Hyperspectral remote sensing using spaceborne, airborne, drone-based, and ground-based sensors will play significant roles in these agricultural, ecological, and biogeological sciences and applications. Interdisciplinary research studies between the disciplines of physics, ecophysiology, and computing technologies can be productive.

ACKNOWLEDGMENTS

This work was supported in part by MEXT, JSPS and CSTI-SIP (NARO), Japan, respectively.

Author contribution: This chapter was conceived and supervised by Inoue. Section 2.6 was written by Darvishzadeh and Skidmore, and all the other sections were written by Inoue.

REFERENCES

Abdullah, H., Darvishzadeh, R., Skidmore, A.K., Groen, T.A., and Heurich, M. 2018. European spruce bark beetle (*Ips typographus*, L.) green attack affects foliar reflectance and biochemical properties. *International Journal of Applied Earth Observation and Geoinformation*, 64, 199–209.

Ali, I., Greifeneder, F., Stamenkovic, J., Neumann, M., and Notarnicola, C. 2015. Review of machine learning approaches for biomass and soil moisture retrievals from remote sensing data. *Remote Sensing*, 7, 16398–16421.

Ali, A.M., Darvishzadeh, R., Skidmore, A.K., and van Duren, I. 2016a. Effects of canopy structural variables on retrieval of leaf dry matter content and specific leaf area from remotely sensed data. *IEEE Journal of Selected Topics in Applied Earth Observations and Remote Sensing*, 9, 898–909.

Ali, A.M., Darvishzadeh, R., Skidmore, A.K., Duren, I. van, Heiden, U., and Heurich, M. 2016b. Estimating leaf functional traits by inversion of PROSPECT: Assessing leaf dry matter content and specific leaf area in mixed mountainous forest. *International Journal of Applied Earth Observation and Geoinformation*, 45, A, 66–76.

Ali, A.M., Skidmore, A.K., Darvishzadeh, R., van Duren, I., Holzwarth, S., and Mueller, J. 2016c. Retrieval of forest leaf functional traits from HySpex imagery using radiative transfer models and continuous wavelet analysis. *ISPRS Journal of Photogrammetry and Remote Sensing*, 122, 68–80.

Ali, A.M., Darvishzadeh, R., and Skidmore, A.K. 2017a. Retrieval of specific leaf area from Landsat-8 surface reflectance data using statistical and physical models. *IEEE Journal of Selected Topics in Applied Earth Observations and Remote Sensing*, 10, 3529–3536.

Ali, A.M., Darvishzadeh, R., Skidmore, A.K., and van Duren, I. 2017b. Specific leaf area estimation from leaf and canopy reflectance through optimization and validation of vegetation indices. *Agricultural and Forest Meteorology*, 236, 162–174.

Asner, G.P., Wessman, C.A., Schimel, D.S., and Archer, S. 1998. Variability in Leaf and Litter Optical Properties: Implications for BRDF Model Inversions Using AVHRR, MODIS, and MISR. *Remote Sensing of Environment*, 63, 243–257.

Asner, G.P. and Martin, R.E. 2009. Airborne spectranomics: Mapping canopy chemical and taxonomic diversity in tropical forests. *Frontiers in Ecology and the Environment*, 7, 269–276.

Asner, G.P., Martin, R.E., Knapp, D.E., Tupayachi, R., Anderson, C., Carranza, L., Martinez, P., Houcheime, M., Sinca, F., and Weiss, P. 2011. Spectroscopy of canopy chemicals in humid tropical forests. *Remote Sensing of Environment*, 115, 3587–3598.

Asrar, G., Myneni, R.B., and Kanemasu, E.T. 1989. Estimation of plant-canopy attributes from spectral reflectance measurements. In: Asrar, G. (Ed.), *Theory and Application of Optical Remote Sensing*. Wiley Interscience, New York, USA, pp. 252–296.

Atzberger, C. 2000. Development of an invertible forest reflectance model: The INFOR-Model, In: Buchroithner, M.F. (Ed.), *A Decade of Trans-European Remote Sensing Cooperation: Proceedings of the 20th EARSeL Symposium*. Dresden, Germany, 14–16 June, 2000, pp. 2039–2044.

Bacour, C., Jacquemoud, S., Tourbier, Y., Dechambre, M., and Frangi, J.P. 2002. Design and analysis of numerical experiments to compare four canopy reflectance models. *Remote Sensing of Environment*, 79, 72–83.

Baret, F. and Guyot, G. 1991. Potentials and limits of vegetation indices for LAI and APAR assessment. *Remote Sensing of Environment*, 35, 161–173.
Baret, F., Houlès, V., and Guérif, M. 2007. Quantification of plant stress using remote sensing observations and crop models: The case of nitrogen management. *Journal of Experimental Botany*, 58, 869–880.
Barton, C.V.M. and North, P.R.J. 2001. Remote sensing of canopy light use efficiency using the photochemical reflectance index—Model and sensitivity analysis. *Remote Sensing of Environment*, 78, 264–273.
Blackburn, G.A. 1998. Quantifying chlorophylls and carotenoids at leaf and canopy scales: An evaluation of some hyperspectral approaches. *Remote Sensing of Environment*, 66, 273–285.
Boegh, E., Soegaard, H., Broge, N., Hasager, C.B., Jensen, N.O., Schelde, K., and Thomsen, A. 2002. Airborne multispectral data for quantifying leaf area index, nitrogen concentration, and photosynthetic efficiency in agriculture. *Remote Sensing of Environment*, 81, 179–193.
Bongiovanni, R. and Lowenberg-Deboer, J. 2004. Precision agriculture and sustainability. *Precision Agriculture*, 5, 359–387.
Broge, N.H. and Leblanc, E. 2000. Comparing prediction power and stability of broadband and hyperspectral vegetation indices for estimation of green leaf area index and canopy chlorophyll density. *Remote Sensing of Environment*, 76, 156–172.
Cadotte, M.W., Carscadden, K., and Mirotchnick, N. 2011. Beyond species: Functional diversity and the maintenance of ecological processes and services. *Journal of Applied Ecology*, 48, 1079–1087.
Cammarano, D., Fitzgerald, G.J., Casa, R., and Basso, B. 2014. Assessing the robustness of vegetation indices to estimate wheat N in Mediterranean environments. *Remote Sensing*, 6, 2827–2844.
Camps-Valls, G., Bruzzone, L., Rojo-Alvarez, J.L., and Melgani, F. 2006. Robust support vector regression for biophysical variable estimation from remotely sensed images. *IEEE Geoscience and Remote Sensing Letters*, 3, 339–343.
Carter, G.A. 1994. Ratios of leaf reflectances in narrow wavebands as indicators of plant stress. *International Journal of Remote sensing*, 15, 697–703.
Castro-Esau, K. L., Sánchez-Azofeifa, G. A., and Rivard, B. 2006. Comparison of spectral indices obtained using multiple spectroradiometers. *Remote Sensing of Environment*, 103, 276–288.
Ceccato, P., Gobron, N., Flasse, S., Pinty, B., and Tarantola, S. 2002. Designing a spectral index to estimate vegetation water content from remote sensing data: Part 2. Validation and applications. *Remote Sensing of Environment*, 82, 198–207.
Cheng, T., Rivard, B., Sánchez-Azofeifa, G.A., Feng, J., and Calvo-Polanco, M. 2010. Continuous wavelet analysis for the detection of green attack damage due to mountain pine beetle infestation. *Remote Sensing of Environment*, 114, 899–910.
Cho, M.A., Skidmore, A.K., and Atzberger, C.G. 2008. Towards red-edge positions less sensitive to canopy biophysical parameters for leaf chlorophyll estimation using properties optique spectrales des feuilles PROSPECT and scattering by arbitrarily inclined leaves SAILH simulated data. *International Journal of Remote Sensing*, 29, 2241–2255.
Choudhury, B.J. 2000. A sensitivity analysis of the radiation use efficiency for gross photosynthesis and net carbon accumulation by wheat. *Agricultural and Forest Meteorology*, 101, 217–234.
Clerbaux, C., Drummond, J.R., Flaud, J.-M., and Orphal, J. 2011. Using thermal infrared absorption and emission to determine trace gases. *The Remote Sensing of Tropospheric Composition from Space*, Springer, pp. 123–151.
Colgan, M.S., Martin, R.E., Baldeck, C.A., and Asner, G.P. 2015. Tree foliar chemistry in an African savanna and its relation to life history strategies and environmental filters. *PLoS One*, 10(5), e0124078.
Combal, B., Baret, F., Weiss, M., Trubuil, A., Macé, D., Pragnère, A., Myneni, R., Knyazikhin, Y., and Wang, L. 2003. Retrieval of canopy biophysical variables from bidirectional reflectance using prior information to solve the ill-posed inverse problem. *Remote Sensing of Environment*, 84, 1–15.
Curran, P.J. 1989. Remote sensing of foliar chemistry. *Remote Sensing of Environment*, 30, 271–278.
Darvishzadeh, R., Skidmore, A., Atzberger, C., and van Wieren, S. 2008a. Estimation of vegetation LAI from hyperspectral reflectance data: Effects of soil type and plant architecture. *International Journal of Applied Earth Observation and Geoinformation*, 10, 358–373.
Darvishzadeh, R., Skidmore, A., Schlerf, M., and Atzberger, C. 2008b. Inversion of a radiative transfer model for estimating vegetation LAI and chlorophyll in a heterogeneous grassland. *Remote Sensing of Environment*, 112, 2592–2604.
Darvishzadeh, R., Atzberger, C., Skidmore, A.K., and Abkar, A.A. 2009. Leaf area index derivation from hyperspectral vegetation indices and the red edge position. *International Journal of Remote Sensing*, 30, 6199–6218.

Dash, J. and Curran, P.J. 2004. The MERIS terrestrial chlorophyll index. *International Journal of Remote Sensing*, 25, 5403–5413.

Daughtry, C.S.T., Gallo, K.P., and Bauer, M.E. 1983. Spectral estimates of Solar radiation intercepted by corn canopies. *Agronomy Journal*, 75, 527–531.

Daughtry, C.S.T., Walthall, C.L., Kim, M.S., de Colstoun, E.B., and McMurtrey, J.E. III. 2000. Estimating corn leaf chlorophyll concentration from leaf and canopy reflectance. *Remote Sensing of Environment*, 74, 229–239.

Dawson, T.P., Curran, P.J., North, P.R.J., and Plummer, S.E. 1999. The propagation of foliar biochemical absorption features in forest canopy reflectance: a theoretical analysis. *Remote Sensing of Environment*, 67, 147–159.

de Leeuw, J., Georgiadou, Y., Kerle, N., de Gier, A., Inoue, Y., Ferwerda, J., Smies, M., and Narantuya, D. 2010. The function of remote sensing in support of environmental policy. *Remote Sensing*, 2, 1731–1750.

De Pury, D.G.G. and Farquhar, G.D. 1997. Simple scaling of photosynthesis from leaves to canopies without the errors of big-leaf models. *Plant, Cell and Environment*, 20, 537–557.

Del Frate, F., Ferrazzoli, P., and Schiavon, G. 2003. Retrieving soil moisture and agricultural variables by microwave radiometry using neural networks. *Remote Sensing of Environment*, 84, 174–183.

Delegido, J., Fernndez, G., Gand, S., and Moreno, J. 2008. Retrieval of chlorophyll content and LAI of crops using hyperspectral techniques: Application to PROBA/CHRIS data. *International Journal of Remote Sensing*, 29, 7107–7127.

Demetriades-Shah, T.H., Steven, M.D., and Clark, J.A. 1990. High resolution derivative spectra in remote sensing. *Remote Sensing of Environment*, 33, 55–64.

Demmig-Adams, B.B. and Adams, W.W. 1996. The role of xanthophyll cycle carotenoids in the protection of photosynthesis. *Trends in Plant Science*, 1, 21–26.

Dobermann, A. and Cassman, K. G. 2004. Environmental dimensions of fertilizer nitrogen: What can be done to increase nitrogen use efficiency and ensure food security? In: Mosier, A.R., Syers, J.K., and Freney, J.R. (Eds.), *Agriculture and the Nitrogen Cycle*. Island Press, Washington, USA, pp. 261–278.

Doktor, D., Lausch, A., Spengler, D., and Thurner, M. 2014. Extraction of plant physiological status from hyperspectral signatures using machine learning methods. *Remote Sensing*, 6, 12247–12274.

Durbha, S.S., King, R.L., and Younan, N.H. 2007. Support vector machines regression for retrieval of leaf area index from multiangle imaging spectroradiometer. *Remote Sensing of Environment*, 107, 348–361.

Feilhauer, H., Somers, B., and van der Linden, S. 2017. Optical trait indicators for remote sensing of plant species composition: Predictive power and seasonal variability. *Ecological Indicators*, 73, 825–833.

Féret, J.-B., François, C., Gitelson, A., Asner, G.P., Barry, K.M., Panigada, C., Richardson, A.D., and Jacquemoud, S. 2011. Optimizing spectral indices and chemometric analysis of leaf chemical properties using radiative transfer modeling. *Remote Sensing of Environment*, 115, 2742–2750.

Ferwerda, J.G., Skidmore, A.K., and Mutanga, O. 2005. Nitrogen detection with hyperspectral normalized ratio indices across multiple plant species. *International Journal of Remote sensing*, 26, 4083–4095.

Field, C. and Mooney, H.A. 1986. The photosynthesis–nitrogen relationship in wild plants, In: Givnish, T.J. (Ed.), *On the Economy of Plant Form and Function*. Cambridge University Press., London, UK, pp. 25–55.

Fourty, T., Baret, F., Jacquemoud, S., Schmuck, G., and Verdebout, J. 1996. Leaf optical properties with explicit description of its biochemical composition: Direct and inverse problems. *Remote Sensing of Environment*, 56, 104–117.

Gamon, J.A., Peñuelas, J., and Field, C.B. 1992. A narrow-waveband spectral index that tracks diurnal changes in photosynthetic efficiency. *Remote Sensing of Environment*, 41, 35–44.

Garbulsky, M.F., Peñuelas, J., Gamon, J., Inoue, Y., and Filella, I. 2010. The photochemical reflectance index (PRI) and the remote sensing of leaf, canopy and ecosystem radiation use efficiencies. *Remote Sensing of Environment*, 115, 281–297.

Gitelson, A.A. and Merzlyak, M.N. 1997. Remote estimation of chlorophyll content in higher plant leaves. *International Journal of Remote Sensing*, 18, 2691–2697.

Gitelson, A.A., Merzlyak, M.N., and Chivkunova, O.B. 2001. Optical properties and nondestructive estimation of anthocyanin content in plant leaves. *Photochemistry and Photobiology*, 74, 38–45.

Gitelson, A.A., Gritz, U., and Merzlyak, M.N. 2003. Relationships between leaf chlorophyll content and spectral reflectance and algorithms for non-destructive chlorophyll assessment in higher plant leaves. *Journal of Plant Physiology*, 160, 271–282.

Gitelson, A.A., Viña, A., Rundquist, D.C., Ciganda, V., and Arkebauer, T.J. 2005. Remote estimation of canopy chlorophyll content in crops. *Geophysical Research Letters*, 32, L08403, doi:10.1029/2005GL022688.

Goetz, S.J., Prince, S.D., Goward, S.N., Thawley, M.M., and Small, J. 1999. Satellite remote sensing of primary production: An improved production efficiency modeling approach. *Ecological Modeling*, 122, 239–255.

Grace, J., Nichol, C., Disney, M., Lewis, P., Quaife, T., and Bowyer, P. 2007. Can we measure terrestrial photosynthesis from space directly, using spectral reflectance and fluorescence? *Global Change Biology*, 13, 1484–1497.

Grossman, Y.L., Ustin, S.L., Jacquemoud, S., Sanderson, E.W., Schmuck, G., and Verdebout, J. 1996. Critique of stepwise multiple linear regression for the extraction of leaf biochemistry information from leaf reflectance data. *Remote Sensing of Environment*, 56, 182–193.

Hall, F.G., Shimabukuro, Y.E., and Huemmrich, K.F. 1995. Remote sensing of forest biophysical structure using mixture decomposition and geometric reflectance models. *Ecological Applications*, 5, 993–1013.

Hansen, P.M. and Schjoerring, J.K. 2003. Reflectance measurement of canopy biomass and nitrogen status in wheat crops using normalized difference vegetation indices and partial least squares regression. *Remote Sensing of Environment*, 86, 542–553.

Hikosaka, K. 2004. Interspecific difference in the photosynthesis-nitrogen relationship: Patterns, physiological causes, and ecological importance. *Journal of Plant Research*, 117(6), 481–494.

Hinzman, L.D., Bauer, M.E., and Daughtry, C.S.T. 1986. Effects of nitrogen fertilization on growth and reflectance characteristics of winter wheat. *Remote Sensing of Environment*, 19, 47–61.

Homolová, L., Malenovský, Z., Clevers, J.G.P.W., García-Santos, G., and Schaepman, M.E. 2013. Review of optical-based remote sensing for plant trait mapping. *Ecological Complex*, 15, 1–16.

Houlès, V., Guérif, M., and Mary, B. 2007. Elaboration of a nitrogen nutrition indicator for winter wheat based on leaf area index and chlorophyll content for making nitrogen recommendations. *European Journal of Agronomy*, 27, 1–11.

Huesca, M., García, M., Roth, K.L., Casas, A., and Ustin, S.L. 2016. Canopy structural attributes derived from AVIRIS imaging spectroscopy data in a mixed broadleaf/conifer forest. *Remote Sensing of Environment*, 182, 208–226.

Huete, A.R. 1988. A soil vegetation adjusted index (SAVI). *Remote Sensing of Environment*, 25, 295–309.

Huete, A.R., Didan, K., Miura, T., Rodriguez, E.P., Gao, X., and Ferreira, L.G. 2002. Overview of the radiometric and biophysical performance of the MODIS vegetation indices. *Remote Sensing of Environment*, 83, 195–213.

Hunt, E.R., Jr. and Rock, B.N. 1989. Detection of changes in leaf water content using near- and middle-infrared reflectances. *Remote Sensing of Environment*, 30, 43–54.

Inada, K. 1985. Spectral ratio of reflectance for estimating chlorophyll content of leaf. *Japanese Journal of Crop Science*, 154, 261–265.

Inoue, Y., Kimball, B.A., Jackson, R.D., Pinter, P.J. Jr., and Reginato, R.J. 1990. Remote estimation of leaf transpiration rate and stomatal resistance based on infrared thermometry. *Agricultural and Forest Meteorology*, 51, 21–33.

Inoue, Y. and Iwasaki, K. 1991. Spectral estimation of radiation absorptance and leaf area index in corn canopies as affected by canopy architecture and growth stage. *Japanese Journal of Crop Science*, 60, 578–580.

Inoue, Y., Morinaga, S., and Shibayama, M. 1993. Non-destructive estimation of water status of intact crop leaves based on spectral reflectance measurements. *Japanese Journal of Crop Science*, 62, 462–469.

Inoue, Y., Moran, M.S., and Horie, T. 1998. Analysis of spectral measurements in Rice paddies for predicting rice growth and yield based on a simple crop simulation model. *Plant Production Science*, 1, 269–279.

Inoue, Y., Kurosu, T., Maeno, H., Uratsuka, S., Kozu, T., Dabrowska-Zielinska, K., and Qi, J. 2002. Season-long daily measurements of multifrequency (Ka, Ku, X, C, and L) and full-polarization backscatter signatures over paddy rice field and their relationship with biological variables. *Remote Sensing of Environment*, 81, 194–204.

Inoue, Y. 2003. Synergy of remote sensing and modeling for estimating ecophysiological processes in plant production. *Plant Production Science*, 6, 3–16.

Inoue, Y. and Olioso, A. 2006. Estimating dynamics of ecosystem CO_2 flux and biomass production in agricultural field by synergy of process model and remotely sensed signature. *Journal of Geophysical Research*, 111(D24), D24S91, doi:10.1029/2006JD007469.

Inoue, Y. and Peñuelas, J. 2006. Relationship between light use efficiency and photochemical reflectance index in soybean leaves as affected by soil water content. *International Journal of Remote Sensing*, 27, 5249–5254.

Inoue, Y., Miah, G., Sakaiya, E., Nakano, K., and Kawamura, K. 2008a. NDSI map and IPLS using hyperspectral data for assessment of plant and ecosystem variables. *Journal of the Remote Sensing Society of Japan*, 28, 1–14.

Inoue, Y., Peñuelas, J., Miyata, A., and Mano, M. 2008b. Normalized difference spectral indices for estimating photosynthetic efficiency and capacity at a canopy scale derived from hyperspectral and CO_2 flux measurements in rice. *Remote Sensing of Environment*, 112, 156–172.

Inoue, Y., Kiyono, Y., Asai, H., Ochiai, Y., Qi, J., Olioso, A., Shiraiwa, T., Horie, T., Saito, K., and Dounagsavanh, L. 2010. Assessing land use and carbon stock in slash-and-burn ecosystems in tropical mountain of Laos based on time-series satellite images. *International Journal of Applied Earth Observation and Geoinformation*, 12, 287–297.

Inoue, Y., Dabrowska-Zierinska, K., and Qi, J. 2012a. Synoptic assessment of environmental impact of agricultural management: A case study on nitrogen fertilizer impact on groundwater quality, using a fine-scale geoinformation system. *International Journal of Environmental Studies*, 69, 443–460.

Inoue, Y., Sakaiya, E., Zhu, Y., and Takahashi, W. 2012b. Diagnostic mapping of canopy nitrogen content in rice based on hyperspectral measurements. *Remote Sensing of Environment*, 126, 210–221.

Inoue, Y., Sakaiya, E., and Wang, C. 2014. Capability of C-band backscattering coefficients from high-resolution satellite SAR sensors to assess biophysical variables in paddy rice. *Remote Sensing of Environment*, 140, 257–266.

Inoue, Y., Guérif, M., Baret, F., Skidmore, A., Gitelson, A., Schlerf, M., Darvishzadeh, R., and Olioso, A. 2016. Simple and robust methods for remote sensing of canopy chlorophyll content: A comparative analysis of hyperspectral data for different types of vegetation. *Plant, Cell and Environment*, 39, 2609–2623.

Inoue, Y. 2017. Remote sensing of plant and soil information by high-resolution optical satellite sensors and its applications to smart agriculture. *Journal of the Remote Sensing Society of Japan*, 37, 213–223.

Inoue, Y. and Yokoyama, M. 2017. Drone-based remote sensing of crops and soils and its application to smart agriculture. *Journal of the Remote Sensing Society of Japan*, 37, 224–235.

IPCC. 2014. Summary for policymakers. In: Field, C.B. and Barros, V.R. et al. (Eds), *Climate Change 2014: Impacts, Adaptation, and Vulnerability. Part A: Global and Sectoral Aspects. Contribution of Working Group II to the Fifth Assessment Report of the Intergovernmental Panel on Climate Change*. Cambridge University Press, Cambridge, UK, pp. 1–32.

Ishijima, K., Sugawara, S., Kawamura, K., Hashida, G., Morimoto, S., Murayama, S., Aoki, S., and Nakazawa, T. 2007. Temporal variations of the atmospheric nitrous oxide concentration and its $\delta^{15}N$ and $\delta^{18}O$ for the latter half of the 20th century reconstructed from firn air analyses. *Journal of Geophysical Research*, 112, D03305, doi:10.1029/2006JD007208.

Jackson, R.D., Idso, S.B., Reginato, R.J., and Pinter, P.J., Jr. 1981. Canopy temperature as a crop water stress indicator. *Water Resources Research*, 17, 1133–1138.

Jacquemoud, S. and Baret, F. 1990. PROSPECT: A model of leaf optical properties spectra. *Remote Sensing of Environment*, 34, 75–91.

Jacquemoud, S., Ustin, S.L., Verdebout, J., Schmuck, G., Andreoli, G., and Hosgood, B. 1996. Estimating leaf biochemistry using the PROSPECT leaf optical properties model. *Remote Sensing of Environment*, 56, 194–202.

Jacquemoud, S., Verhoef, W., Baret, F., Bacour, C., Zarco-Tejada, P.J., Asner, G.P., François, C., and Ustin, S.L. 2009. PROSPECT+SAIL: A review of use for vegetation characterization. *Remote Sensing of Environment*, 113, S56–S66.

Jongschaap, R.E. and Booij, R. 2004. Spectral measurements at different spatial scales in potato: Relating leaf, plant and canopy nitrogen status. *International Journal of Applied Earth Observation and Geoinformation*, 5, 204–218.

Karnieli, A., Bayarjargal, Y., Bayasgalan, M., Mandakh, B., Dugarjav, Ch., Burgheimer, J., Khudulmur, S., Bazha, S.N., and Gunin, P.D. 2013. Do vegetation indices provide a reliable indication of vegetation degradation? A case study in the Mongolian pastures. *International Journal of Remote Sensing*, 34, 6243–6262.

Kiniry, J.R., Jones, C.A., O'Toole, J.C., Blanchet, R., Cabelguenne, M., and Spanel, D.A. 1989. Radiation-use efficiency in biomass accumulation prior to grain-filling for five grain-crop species. *Field Crops Research*, 20, 51–64.

Kljun, N., Kastner-Klein, P., Fedorovich, E., and Rotach, M.W. 2004. Evaluation of Lagrangian footprint model using data from wind tunnel convective boundary layer. *Agricultural and Forest Meteorology*, 127, 189–201.

Knyazikhin, Y., Lewis, P., Disney, M.I., Stenberg, P., Mottus, M., Rautiainen, M., Kaufmann, R.K. et al. 2013. Reply to Townsend et al.: Decoupling contributions from canopy structure and leaf optics is critical for remote sensing leaf biochemistry. *Proceedings of the National Academy of Sciences*, 110, E1075–E1075.

Kokaly, R.F., Asner, G.P., Ollinger, S.V., Martin, M.E., and Wessman, C.A. 2009. Characterizing canopy biochemistry from imaging spectroscopy and its application to ecosystem studies. *Remote Sensing of Environment*, 113, S78–S91.

Kumar, M. and Monteith, J.L. 1982. Remote sensing of crop growth. In: Smith, H. (Ed.), *Plants and the Daylight Spectrum*. Academic Press, London, UK, pp. 133–144.

Kuusk, A. 1991. The hot-spot effect in plant canopy reflectance. In: R.B. Myneni and J. Ross (Eds.), *Photon–Vegetation Interactions*. Springer-Verlag, New York, USA, pp. 139–159.

Lal, B., Balakrishnan, A., Picard, A., Corbin, B., Behrens, J., Green, E., and Myers, R. 2017. *Trends in small satellite technology and the role of the NASA small spacecraft technology program*. Report of Science and Technology Policy Institute. https://www.nasa.gov/sites/default/files/atoms/files/nac_march2017_blal_ida_sstp_tagged.pdf. (Accessed December 15, 2017)

Lavorel, S., Grigulis, K., Lamarque, P., Colace, M., Garden, D., Girel, J., Pellet, G., and Douzet, R. 2011. Using plant functional traits to understand the landscape distribution of multiple ecosystem services. *Journal of Ecology*, 99, 135–147.

Leardi, R. and Norgaard, L. 2004. Sequential application of backward interval partial least squares and genetic algorithms for the selection of relevant spectral regions. *Journal of Chemometrics*, 18, 486–497.

Lee, Y., Yang, C., Chang, K., and Shen, Y. 2008. A simple spectral index using reflectance of 735 nm to assess nitrogen status of rice canopy. *Agronomy Journal*, 100, 205–212.

Lefsky, M.A., Cohen, W.B., Acker, S.A., Parker, G.G., Spies, T.A., and Harding, D. 1999. Lidar remote sensing of the canopy structure and biophysical properties of douglas-fir Western Hemlock forests. *Remote Sensing of Environment*, 70, 339–361.

le Maire, G., François, C., Soudani, K., Berveiller, D., Pontailler, J.Y., Bréda, N., Genet, H., Davi, H., and Dufrêne, E. 2008. Calibration and validation of hyperspectral indices for the estimation of broadleaved forest leaf chlorophyll content, leaf mass per area, leaf area index and leaf canopy biomass. *Remote Sensing of Environment*, 112, 3846–3864.

Le Toan, T., Ribbes, F., Wang, L.F., Nicolas, F., Ding, K.H., Kong, J.A., Fujita, M., and Kurosu, T. 1997. Rice crop mapping and monitoring using ERS-1 data based on experiment and modeling results. *IEEE Transactions on Geoscience and Remote Sensing*, 35, 41–56.

Liu, W., Baret, F., Gu, X., Zhang, B., Tong, Q., and Zheng, L. 2003. Evaluation of methods for soil surface moisture estimation from reflectance data. *International Journal of Remote Sensing*, 24, 2069–2083.

Lloyd, J., Bloomfield, K., Domingues, T.F., and Farquhar, G.D. 2013. Photosynthetically relevant foliar traits correlating better on a mass vs an area basis: Of ecophysiological relevance or just a case of mathematical imperatives and statistical quicksand? *New Phytologist*, 199, 311–321.

Martin, M.E., Plourde, L.C., Ollinger, S.V., Smith, M.-L., and McNeil, B.E. 2008. A generalizable method for remote sensing of canopy nitrogen across a wide range of forest ecosystems. *Remote Sensing of Environment*, 112, 3511–3519.

Meroni, M., Colombo, R., and Panigada, C. 2004. Inversion of a radiative transfer model with hyperspectral observations for LAI mapping in poplar plantations. *Remote Sensing of Environment*, 92, 195–206.

Ministry of Agriculture, Fisheries and Food of UK (MAFF-UK) 2000. *Fertilizer Recommendations for Agricultural and Horticultural crops* (RB209). 7th Edn., 1–175pp.

Mirzaie, M., Darvishzadeh, R., Shakiba, A., Matkan, A.A., Atzberger, C., and Skidmore, A. 2014. Comparative analysis of different uni- and multi-variate methods for estimation of vegetation water content using hyperspectral measurements. *International Journal of Applied Earth Observation and Geoinformation*, 26, 1–11.

Monsi, M. and Saeki, T. 1953. Uber den Lichtfactor in den Pflanzengesellshaften und seine Bedeutung fur dir Stoffproduktion. *Japanese Journal of Botany*, 14, 22–52.

Monteith, J.L. 1977. Climate and the efficiency of crop production in Britain. *Philosophical Transactions of the Royal Society of London B*, 281, 277–294.

Moran, M.S., Clarke, T.R., Inoue, Y., and Vidal, A. 1994. Estimating crop water deficit using the relation between surface-air temperature and spectral vegetation index. *Remote Sensing of Environment*, 49, 246–263.

Moran, M.S., Inoue, Y., and Barnes, E.M. 1997. Opportunities and limitations for image-based remote sensing in precision crop management. *Remote Sensing of Environment*, 61, 319–346.

Morita, K. 1978. A physiological study on the dynamic status of leaf nitrogen in rice plants. *Bulletin of Hokuriku Agricultural Experimental Station*, 21, 1–61.

Muñoz-Huerta, R.F., Guevara-Gonzalez, R.G., Contreras-Medina, L.M., Torres-Pacheco, I., Prado-Olivarez, J., and Ocampo-Velazquez, R. V. 2013. A review of methods for sensing the nitrogen status in plants: Advantages, disadvantages and recent advances. *Sensors*, 13, 10823–10843.

Mutanga, O. and Skidmore, A.K. 2004. Narrow band vegetation indices overcome the saturation problem in biomass estimation. *International Journal of Remote Sensing*, 25, 3999–4014.

Mutanga, O. and Skidmore, A.K. 2007. Red edge shift and biochemical content in grass canopies. *ISPRS Journal of Photogrammetry and Remote Sensing*, 62(1), 34–42.

Myneni, R.B. and Williams, D.L. 1994. On the relationship between FAPAR and NDVI. *Remote Sensing of Environment*, 49, 200–211.

Naesset, E., Bollandsas, O.M., and Gobakken, T. 2005. Comparing regression methods in estimation of biophysical properties of forest stands from two different inventories using laser scanner data. *Remote Sensing of Environment*, 94, 541–553.

Nagendra, H., Lucas, R., Honrado, J.P., Jongman, R.H.G., Tarantino, C., Adamo, M., and Mairota, P. 2013. Remote sensing for conservation monitoring: Assessing protected areas, habitat extent, habitat condition, species diversity, and threats. *Ecological Indicators*, 33, 45–59.

Neinavaz, E., Skidmore, A.K., Darvishzadeh, R., and Groen, T.A. 2016a. Retrieval of leaf area index in different plant species using thermal hyperspectral data. *ISPRS Journal of Photogrammetry and Remote Sensing*, 119, 390–401.

Neinavaz, E., Skidmore, A.K., Darvishzadeh, R., and Groen, T.A. 2016b. Leaf area index retrieved from thermal hyperspectral data. ISPRS Commission VII, WG VII/3. *International Archives of the Photogrammetry, Remote Sensing and Spatial Information Sciences—ISPRS Archives*, 99–105.

Neinavaz, E., Darvishzadeh, R., Skidmore, A. K., and Groen, T. A. 2016c. Measuring the response of canopy emissivity spectra to leaf area index variation using thermal hyperspectral data. *International Journal of Applied Earth Observation and Geoinformation*, 53, 40–47.

Nishio, M. 2005. *Agriculture and Environmental Pollution—Technology and Policy for Soil Environment -*. Rural Culture Association, Tokyo, Japan, 439pp.

Nobel, P.S. 2005. *Physicochemical and Environmental Plant Physiology* (3rd Ed.). Elsevier Academic Press, Amsterdam, Netherlands, 567pp.

Norgaard, L., Saudland, A., Wagner, J., Nielsen, J.P., Munck, L., and Engelsen, S.B. 2000. Interval partial least-squares regression (iPLS): A comparative chemometric study with an example from near-infrared spectroscopy. *Applied Spectroscopy*, 54, 413–419.

Notarnicola, C., Angiulli, M., and Posa, F. 2008. Soil moisture retrieval from remotely sensed data: Neural network approach versus Bayesian method. *IEEE Transactions on Geoscience and Remote Sensing*, 46, 547–557.

Nouvellon, Y., Seen, D.L., Rambal, S., Begue A., Moran, M.S., Kerr, Y., and Qi, J. 2000. Time course of radiation use efficiency in a shortgrass ecosystem: Consequences for remotely sensed estimation of primary production. *Remote Sensing of Environment*, 71, 43–55.

Ollinger, S. V., Richardson, A.D., Martin, M.E., Hollinger, D.Y., Frolking, S.E., Reich, P.B., Plourde, L.C. et al. 2008. Canopy nitrogen, carbon assimilation, and albedo in temperate and boreal forests: Functional relations and potential climate feedbacks. *Proceedings of the National Academy of Sciences*, 105, 19336–19341.

Olioso, A., Inoue, Y., Ortega-Farias, S., Demarty, J., Wigneron, J-P. Braud, T., Jacob, F. et al. 2005. Future directions for advanced evapotranspiration modeling: Assimilation of remote sensing data into crop simulation models and SVAT models. *Irrigation and Drainage Systems*, 19, 377–412.

Peñuelas, J., Filella, I., and Gamon, J.A. 1995. Assessment of plant photosynthetic radiation-use efficiency with spectral reflectance. *New Phytologist*, 131, 291–296.

Peñuelas J., Filella I. 1998. Visible and near-infrared reflectance techniques for diagnosing plant physiological status. *Trends in Plant Science*, 3, 151–156.

Peñuelas, J. and Inoue, Y. 1999. Reflectance indices indicative of changes in water and pigment content of peanut and wheat leaves. *Photosynthetica*, 36, 355–360.

Pereira, H.M., Ferrier, S., Walters, M., Geller, G.N., Jongman, R.H.G., Scholes, R.J., Bruford, M.W. et al. 2013. Essential biodiversity variables. *Science*, 80–339, 277–278.

Pierce, L., Running, S.W., and Walker, J. 1994. Regional-scale relationships of leaf area index to specific leaf area and leaf nitrogen content. *Ecological Applications*, 313–321.

Pinter, P.J., Jackson, R.D., Ezra, C.E., and Gausman, H.W. 1985. Sun angle and canopy architecture effects on the reflectance of six wheat cultivars. *International Journal of Remote Sensing*, 6, 1813–1825.

Potter, C.S., Randerson, J.T., Field, C.B., Matson, P.A., Vitousek, P.M., Mooney, H.A., and Klooster, S.A. 1993. Terrestrial ecosystem production: A process model based on global satellite and surface data. *Global Biogeochemical Cycles*, 7, 811–841.

Qi, J., Chehbouni, A., Huete, A.R., Kerr, Y.H., and Sorooshian, S. 1994. A modified soil adjusted vegetation index. *Remote Sensing of Environment*, 48, 119–126.

Qi, J., Inoue, Y., and Wiangwang, N. 2012. Hyperspectral remote sensing in global change studies. In: Thenkabail, P.S., Lyon, J.G., and Huete, A. (Eds.), *Hyperspectral Remote Sensing of Vegetation*. CRC Press, New York, USA, pp. 70–89.

Quattrochi, D.A. and Luvall, J.C. 1999. Thermal infrared remote sensing for analysis of landscape ecological processes: Methods and applications. *Landscape Ecology*, 14, 577–598.

Ribeiro da Luz, B. and Crowley, J.K. 2010. Spectral reflectance and emissivity features of broad leaf plants: Prospects for remote sensing in the thermal infrared (8.0–14.0 μm). *Remote Sensing of Environment*, 109, 393–405.

Richardson, A.D., Duigan, S.P., and Berlyn, G.P. 2002. An evaluation of noninvasive methods to estimate foliar chlorophyll content. *New Phytologist*, 153, 185–194.

Roberto, C., Lorenzo, B., Michele, M., Micol, R., and Cinzia, P. 2012. Optical remote sensing of vegetation water content. In: Thenkabail, P.S., Lyon, J.G., and Huete, A. (Eds.), *Hyperspectral Remote Sensing of Vegetation*. CRC Press, New York, USA, pp. 227–244.

Romero, A., Aguado, I., and Yebra, M. 2012. Estimation of dry matter content in leaves using normalized indexes and PROSPECT model inversion. *International Journal of Remote Sensing*, 33, 396–414.

Rondeaux, G., Steven, M., and Baret, F. 1996. Optimization of soil-adjusted vegetation indices. *Remote Sensing of Environment*, 55, 95–107.

Roosjen, P.P.J., Suomalainen, J.M., Bartholomeus, H.M., Kooistra, L., and Clevers, J.G.P.W. 2017. Mapping reflectance anisotropy of a potato canopy using aerial images acquired with an unmanned aerial vehicle. *Remote Sensing*, 9, 417.

Rosati, A., Day, K.R., and DeJong, T.M. 2000. Distribution of leaf mass per unit area and leaf nitrogen concentration determine partitioning of leaf nitrogen within tree canopies. *Tree Physiology*, 20, 271–276.

Rouse, J.W., Haas, R.H. Jr, Schell, J.A., and Deering, D.W. 1974. Monitoring vegetation systems in the Great Plains with ERTS. *Third ERTS-1 Symposium*, Washington, DC: NASA, 09–317.

Roy, J., Saugier, B., and Mooney, A.H. (Eds.) 2001. *Terrestrial Global Productivity*. Academic Press, London, UK, 573pp.

Ruimy, A., Saugier, B., and Dedieu, G. 1994. Methodology for the estimation of terrestrial net primary production from remotely sensed data. *Journal of Geophysical Research*, 99, 5263–5283.

Sakaiya, E. and Inoue, Y. 2013. Operational use of remote sensing for harvest management of rice. *Journal of The Remote Sensing Society of Japan*, 33(3), 185–199.

Schlerf, M. and Atzberger, C. 2006. Inversion of a forest reflectance model to estimate structural canopy variables from hyperspectral remote sensing data. *Remote Sensing of Environment*, 100, 281–294.

Shibayama, M. and Akiyama, T. 1986. A spectroradiometer for field use. VI. Radiometric estimation for chlorophyll index of rice canopy. *Japanese Journal of Crop Science*, 55, 433–438.

Shibles, R.M. and Weber, R.C. 1966. Interception of solar radiation and dry matter production by various soybean planting patterns. *Crop Science*, 6, 55–59.

Sims, D.A. and Gamon, J.A. 2002. Relationships between leaf pigment content and spectral reflectance across a wide range of species, leaf structures and developmental stages. *Remote Sensing of Environment*, 81, 337–354.

Sinclair, T.R. 1994. Limits to crop yield? In: Boote, K.J., Bennet, J.M., Sinclair, T.R., and Paulsen, G.M. (Eds.), *Physiology and Determination of Crop Yield*. American Society of Agronomy, Madison, WI, USA, pp. 509–532.

Skidmore, A.K., Pettorelli, N., Coops, N.C., Geller, G.N., Hansen, M., Lucas, R., Mücher, C.A. et al. 2015. Environmental science: Agree on biodiversity metrics to track from space. *Nature*, 523, 403–405.

Spiegelman, C.H., McShane, M.J., Goetz, M.J., Motamedi, M., Yue, Q.L., and Coté, G.L. 1998. Theoretical justification of wavelength selection in PLS calibration: Development of a new algorithm. *Analytical Chemistry*, 70, 35–44.

Sripada, R.P., Schmidt, J.P., Dellinger, A.E., and Beegle, D.B. 2008. Evaluating multiple indices from a canopy reflectance sensor to estimate corn N requirements. *Agronomy Journal*, 100, 1553–1561.

Staenz, K. and Held, A. 2012. Summary of current and future terrestrial civilian hyperspectral spaceborne systems. *Proceeding of IEEE International Geoscience and Remote Sensing Symposium (IGARSS) 2012*, July 22–27, 2012, Munich, Germany, 123–125.

Stafford, J.V. 2000. Implementing precision agriculture in the 21st century. *Journal of Agricultural Engineering Research*, 76, 267–275.

Stöcker, C., Bennett, R., Nex, F., Gerke, M., and Zevenbergen, J. 2017. Review of the current state of UAV regulations. *Remote Sensing*, 9, 459.

Takahashi, W., Nguyen-Cong, V., Kawaguchi, S., and Minamiyama, M. 2000. Statistical models for prediction of dry weight and nitrogen accumulation based on visible and near-infrared hyper-spectral reflectance of rice canopies. *Plant Production Science*, 3, 377–386.

Thapa, R.B., Watanabe, M., Motohka, T., and Shimada, M. 2015. Potential of high-resolution ALOS–PALSAR mosaic texture for aboveground forest carbon tracking in tropical region. *Remote Sensing of Environment*, 160, 122–133.

Thenkabail, P.S., Lyon, J.G. and Huete, A. (Eds.) 2012. *Hyperspectral Remote Sensing of Vegetation*. CRC Press, New York, USA, 705pp.

Tilman, D. 2001. Functional Diversity. In: Levin, S.A. (Ed.), *Encyclopedia of Biodiversity*. Academic Press, Oxford, UK, pp. 109–120.

Turner, D.P., Gower, S.T., Stith, T., Cohen, W.B., Gregory, M., and Maiersperger, T.K. 2002. Effects of spatial variability in light use efficiency on satellite-based NPP monitoring. *Remote Sensing of Environment*, 80, 379–406.

Ustin, S.L., Gitelson, A.A., Jacquemoud, S., Schaepman, M., Asner, G.P., Gamon, J.A., and Zarco-Tejada, P. 2009. Retrieval of foliar information about plant pigment systems from high resolution spectroscopy. *Remote Sensing of Environment*, 113, 67–77.

Ustin, S.L. 2013. Remote sensing of canopy chemistry. *Proceedings of the National Academy of Sciences*, 110, 804–805.

Vadrevu, K., Ohara, T., and Justice, C. (Eds.) 2018. *Land-Atmospheric Interactions in Asia*. Springer & Cham, Cham, Switzerland, 500pp.

Verhoef, W. 1984. Light scattering by leaf layers with application to canopy reflectance modeling: The SAIL model. *Remote Sensing of Environment*, 16(2), 125–141.

Verhoef, W. 1985. Earth observation modeling based on layer scattering matrices. *Remote Sensing of Environment*, 17(2), 165–178.

Verhoeven, G. 2011. Taking computer vision aloft—Archaeological three-dimensional reconstructions from aerial photographs with photoscan. *Archaeological Prospection*, 18, 67–73.

Vogelmann, J.E., Rock, B.N., and Moss, D.M. 1993. Red edge spectral measurements from sugar maple leaves. *International Journal of Remote Sensing*, 14, 1563–1575.

Wang, S.H., Ji, Z.J., Liu, S.H., Ding, Y.F., and Cao, W.X. 2003. Relationships between balance of nitrogen supply-demand and nitrogen translocation and senescence of different position leaves on rice. *Agricultural Sciences in China*, 2, 747–751.

Wang, Z., Skidmore, A.K., Darvishzadeh, R., Heiden, U., Heurich, M., and Wang, T. 2015a. Leaf nitrogen content indirectly estimated by leaf traits derived from the PROSPECT model. *IEEE Journal of Selected Topics in Applied Earth Observations and Remote Sensing*, 8, 3172–3182.

Wang, Z., Skidmore, A.K., Wang, T., Darvishzadeh, R., and Hearne, J. 2015b. Applicability of the PROSPECT model for estimating protein and cellulose + lignin in fresh leaves. *Remote Sensing of Environment*, 168, 205–218.

Wang, Z., Skidmore, A.K., Wang, T., Darvishzadeh, R., Heiden, U., Heurich, M., Latifi, H., and Hearne, J. 2017. Canopy foliar nitrogen retrieved from airborne hyperspectral imagery by correcting for canopy structure effects. *International Journal of Applied Earth Observation and Geoinformation*, 54, 84–94.

Wright, I.J., Reich, P.B., Westoby, M., Ackerly, D.D., Baruch, Z., Bongers, F., Cavender-Bares, J. et al. 2004. The worldwide leaf economics spectrum. *Nature*, 428, 821–827.

Xiao, Y., Zhao, W., Zhou, D., and Gong, H. 2014. Sensitivity analysis of vegetation reflectance to biochemical and biophysical variables at leaf, canopy, and regional scales. *IEEE Transactions on Geoscience and Remote Sensing*, 52, 4014–4024.

Yoder, B.J. and Pettigrew-Crosby, R.E. 1995. Predicting nitrogen and chlorophyll content and concentration from reflectance spectra (400–2500 nm) at leaf and canopy scales. *Remote Sensing of Environment*, 53, 199–211.

Zarco-Tejada, P.J., Miller, J.R., Noland, T.L., Mohammed, G.H., and Sampson, P.H. 2001. Scaling-up and model inversion methods with narrowband optical indices for chlorophyll content estimation in closed forest canopies with hyperspectral data. *IEEE Transactions on Geoscience and Remote Sensing*, 39, 1491–1507.

Zarco-Tejada, P.J., Miller, J.R., Mohammed, G.H., Noland, T.L., and Sampson, P.H. 2002. Vegetation stress detection through chlorophyll a + b estimation and fluorescence effects on hyperspectral imagery. *Journal of Environmental Quality*, 31, 1433–1441.

Zhang, C. and Kovacs, J.M. 2012. The application of small unmanned aerial systems for precision agriculture: A review. *Precision Agriculture*, 13, 693–712.

Zhu, Y., Yao, X., Tian, Y., Liu, X., and Cao, W. 2008. Analysis of common canopy vegetation indices for indicating leaf nitrogen accumulations in wheat and rice. *International Journal of Applied Earth Observation and Geoinformation*, 10, 1–10.